



HAL
open science

Bilateral fastigial control of interceptive saccades: evidence from the ipsipulsion of vertical saccades after caudal fastigial inactivation

Clara Bourrelly, Julie Quinet, Laurent Goffart

► **To cite this version:**

Clara Bourrelly, Julie Quinet, Laurent Goffart. Bilateral fastigial control of interceptive saccades: evidence from the ipsipulsion of vertical saccades after caudal fastigial inactivation. 2021. hal-03168070v1

HAL Id: hal-03168070

<https://hal.science/hal-03168070v1>

Preprint submitted on 12 Mar 2021 (v1), last revised 2 Apr 2021 (v2)

HAL is a multi-disciplinary open access archive for the deposit and dissemination of scientific research documents, whether they are published or not. The documents may come from teaching and research institutions in France or abroad, or from public or private research centers.

L'archive ouverte pluridisciplinaire **HAL**, est destinée au dépôt et à la diffusion de documents scientifiques de niveau recherche, publiés ou non, émanant des établissements d'enseignement et de recherche français ou étrangers, des laboratoires publics ou privés.

1 Bilateral fastigial control of interceptive saccades:
2 evidence from the ipsipulsion of vertical saccades after
3 caudal fastigial inactivation

4
5 Clara Bourrelly*, Julie Quinet and Laurent Goffart*

6 Aix Marseille Université, Centre National de la Recherche Scientifique,

7 Institut de Neurosciences de la Timone, Marseille, France.

8
9 Laurent Goffart : <https://orcid.org/0000-0001-8767-1867>

10 Julie Quinet : <https://orcid.org/0000-0003-3043-3424>

11 Title for running head: Neural control of interceptive saccades

12
13 *: C. Bourrelly and L. Goffart contributed equally to this work.

14 Address for correspondence:

15 Laurent Goffart, PhD,

16 E-mail: laurent.goffart@univ-amu.fr

17 Institut de Neurosciences de la Timone, Campus de Sante, 27 Bd Jean Moulin, 13385 Marseille

18 cedex 5, France.

19

20

21 **Abstract (250 words <= 250 words)**

22 During the last decades, the concept was spread that saccades toward a visual target are the
23 outcome of a process transforming the locus of retinal activity into a discharge whose duration
24 determines saccade duration. A “gaze velocity” command would be extracted from target-
25 related signals and sent to the motoneurons while a feedback loop would reduce the mismatch
26 between neurally-encoded target and gaze directions. A different viewpoint has been proposed
27 in which a saccade is the physical outcome of a process that, under cerebellar control, restores
28 the equilibrium of bilateral activity in the brainstem. According to this hypothesis, saccade
29 velocity is not directly encoded within the firing rate of neurons in the brainstem. We further
30 developed this hypothesis by testing, in two head-restrained macaques, the effects of
31 unilaterally inactivating the caudal fastigial nucleus on saccades toward a target moving
32 vertically with a constant, increasing or decreasing speed. After local muscimol injection,
33 vertical saccades were deviated horizontally toward the injected side. The magnitude of this
34 ipsipulsion depended upon the tested target speed, but not its instantaneous value because it did
35 not increase (decrease) when the target accelerated (decelerated). By subtracting the effect on
36 contralesional horizontal saccades from the effect on ipsilesional ones, we found that the net
37 bilateral effect on horizontal saccades was strongly correlated with the effect on vertical
38 saccades. We explain how this correlation corroborates the bilateral hypothesis while raising
39 numerous concerns about the putative encoding of saccade velocity within the discharge of
40 neurons in the brainstem and oculomotor vermis.

41

42 **NEW & NOTEWORTHY (73 <= 75 words)**

43 Besides causing dysmetric horizontal saccades, unilateral inactivation of caudal fastigial
44 nucleus causes an ipsipulsion of vertical saccades. This study is the first to quantitatively
45 describe this ipsipulsion during saccades toward a moving target. By subtracting the effects on
46 contralesional (hypometric) and ipsilesional (hypermetric) horizontal saccades, we find that this
47 net bilateral effect is strongly correlated with the ipsipulsion of vertical saccades, corroborating
48 the suggestion that a common disorder affects all saccades.

49

50 **Introduction**

51 Saccades are rapid changes in eye orientation whose time course is characterized by an
52 interval during which the rotation speed increases to a maximum (acceleration) followed by an
53 interval during which it returns to zero (deceleration). Starting with the eyes centered in the
54 orbits, the changes in the contraction of lateral and medial recti muscles rotate the eyes
55 horizontally whereas combined changes in the contraction of superior and inferior recti
56 muscles, and the superior and inferior oblique muscles rotate them vertically (Robinson 1975).
57 During vertical saccades, the tension in muscles involved in horizontal rotations exhibit a
58 transient small reduction at the level of medial recti (Miller and Robins 1992). A burst of spikes
59 from motoneurons causes the phasic contraction of agonist muscles while the relaxation of
60 antagonist muscles is enabled by a pause of motoneurons which innervate them (Fuchs and
61 Luschei 1970; Robinson 1970; Schiller 1970). Premotor commands for horizontal and vertical
62 eye rotations originate in distinct regions of the reticular formation: burst neurons in the
63 pontomedullary reticular formation drive horizontal saccades whereas those controlling vertical
64 saccades are located in the rostral midbrain tegmentum (Fuchs et al. 1985; Hepp et al., 1989;
65 Horn 2006; Moschovakis et al. 1996).

66 Robinson and Fuchs (2001) proposed that these populations of premotor neurons and
67 the time course of saccades are under the control of neurons in the medio-posterior cerebellum:
68 burst neurons in the contralateral caudal fastigial nucleus (cFN) would support the acceleration
69 of saccades while those in the ipsilateral cFN would help their deceleration. This biphasic
70 pattern was suggested by the delay between the peaks of cFN discharge during contralateral
71 and ipsilateral saccades (Fuchs et al. 1993; Ohtsuka and Noda 1991; Kleine et al. 2003).
72 Moreover, after unilateral cFN inactivation, contralesional saccades are hypometric and exhibit
73 lower peak velocity whereas ipsilesional saccades are hypermetric with a longer deceleration

74 (Buzunov et al. 2013; Goffart et al. 2004). Thus, it was suggested that a shift of activity from
75 the contralateral to the ipsilateral cFN would guide the trajectory of saccades (Optican 2005).

76 Numerous observations lead to questioning this isomorphism which was assumed
77 between the brainstem activity and the kinematics of saccades. Firstly, Davis-Lopez de
78 Carrizosa et al. (2011) showed that a model factoring muscle tension and its first derivative
79 accounted for the firing rate of motoneurons better than a model factoring eye position and its
80 first and second derivatives (velocity and acceleration). Secondly, the resemblance between the
81 firing rate of premotor burst neurons and saccade instantaneous velocity (see for example Fig.
82 5B of Cromer and Waitzman (2007)) disappears when the spikes are not convolved with a
83 Gaussian kernel (see Figs. 2 and 3 in Hu et al. (2007); see also Fig. 4 in van Gisbergen et al.
84 (1981)). Thirdly, the inspection of cFN bursts reveals that the transition between the activity of
85 the left and right cFN is not as sharp as the separation between the acceleration and deceleration
86 phases. In fact, the bursts in the two nuclei largely overlap around the time of saccade peak
87 velocity (Kleine et al. 2003). Moreover, some neurons burst after saccade onset during large
88 contralateral head unrestrained gaze shifts, casting doubt on the cFN's role in accelerating
89 saccades (Fuchs et al. 2010). Involvement in only decelerating ipsilateral saccades is also called
90 into question by the changes in the acceleration of saccades after cFN inactivation (Buzunov et
91 al. 2013; Quinet and Goffart 2007). Finally, a horizontal deviation (ipsipulsion) affects the full
92 time course of vertical saccades, including both acceleration and deceleration, following
93 unilateral cFN inactivation (Goffart et al. 2004; Iwamoto and Yoshida 2002; Quinet and Goffart
94 2007).

95 The hypothesis that cFN activity helps to accelerate contralateral horizontal saccades
96 and to decelerate ipsilateral ones does not explain why vertical saccades exhibit this ipsipulsion.
97 Robinson et al. (1993) proposed a different explanation: “during saccades to vertical targets,
98 there is activity in the horizontal burst generator on one side that is not balanced by activity on

99 the other. Such unbalanced activity might arise because in the normal animal, caudal fastigial
100 neurons on each side burst at about the same time during vertical saccades”. Emphasizing the
101 bilateral organization of cFN efferences to premotor burst neurons (Sparks and Barton 1993)
102 and the bilateral control of saccades (van Gisbergen et al. 1981), Goffart et al. (2004) went
103 further by proposing that the unbalanced activity accounts for the dysmetria of all saccades
104 during cFN unilateral inactivation, regardless of whether the saccade is horizontal, oblique, or
105 vertical. According to this bilateral hypothesis, both cFN influence the premotor process, from
106 saccade onset to saccade end. Regardless of its direction, the saccade is influenced by the
107 discharge from both cFN. If the causes are the same, the ipsipulsion of vertical saccades should
108 be correlated with the dysmetria of horizontal (ipsilesional and contralesional) saccades; this
109 inference is not deducible from the scheme proposed by Robinson and Fuchs (2001). In the
110 present study, we characterize the ipsipulsion of vertical saccades, and confirm this prediction
111 using saccades toward a moving target as a probe. We investigated such saccades because they
112 offer the methodological advantage of enabling to vary both target eccentricity and the saccade
113 amplitude more easily than saccades toward static targets. Goffart et al. (2004) indeed found
114 that the magnitude of the ipsipulsion increased when target eccentricity (see also Iwamoto and
115 Yoshida 2002) or saccade duration increased. Which of these features (target eccentricity or
116 saccade duration) determines the size of the horizontal error could not be determined from their
117 data. Our results do not support a link between the ipsipulsion and saccade duration because
118 across all our testing conditions, its magnitude was less frequently dependent upon the duration
119 than upon the amplitude of vertical saccades.

120 **Materials and Methods**

121 The materials and methods used in this work are identical to those described in Burrelly
122 et al. (2018a, b) and comply with the ARRIVE (Animal Research: Reporting of In Vivo
123 Experiments) guidelines. We will remind them only briefly.

124 *Subjects and surgical procedures*

125 Two adult male rhesus monkeys (*Macaca mulatta*, 11-12 kg) participated in this study.
126 Their eye movements were recorded with the electromagnetic induction technique. Training to
127 the eye movement tasks started after full recovery (> 1 month after surgery). A craniotomy was
128 made to permit the electrophysiological localization of saccade-related neurons in both fastigial
129 nuclei. The surgical procedures and experiments were performed in accordance with the
130 guidelines from the French Ministry of Agriculture and the European Community, after
131 approval from the Regional Ethics Committee (authorization # A13/01/13). Care and
132 maintenance of animals were made under the auspices of a veterinarian and the assistance of
133 animal facilities staff.

134 *Eye movement recording and visual stimulation*

135 During the experimental sessions, the monkeys were seated in a chair with their head
136 restrained, facing a LCD video monitor (Samsung SyncMaster, P227f; 1,280 × 1,024 pixels,
137 100-Hz refresh rate, 39 × 29 cm) located at a viewing distance of 38 cm. The visual target was
138 a Gaussian blurred white disk of 0.4° diameter displayed over a gray background. Eye
139 movements were measured with a phase-angle detection system (CNC Engineering, 3-ft. coil
140 frame) and voltage signals encoding the horizontal and vertical positions of one eye were
141 sampled at 500 Hz. The triggering of stimuli, the on-line recording of the oculomotor
142 performance and the data acquisition were controlled by a PC using the Beethoven software

143 package (Ryklin Software). Eye position signals were calibrated by having the animal fixate
144 stationary targets presented at $\pm 16^\circ$ along the horizontal or vertical meridians.

145 *Oculomotor tests*

146 The experiments were performed more than one year after the monkeys were tested and
147 trained to make saccades toward moving targets (Quinet and Goffart 2015; Burreilly et al.
148 2014, 2016). Each experiment consisted of several pre-injection (control) sessions and one post-
149 injection session. During the control sessions, the eye movements were recorded with a series
150 of trials performed over 3-4 successive days before the injection whereas the post-injection
151 session consisted of recordings made during trials collected approximately 30-50 minutes after
152 the muscimol was injected in the cFN (after removing the cannula from the brain and recording
153 saccades toward static targets). Each trial started with a brief tone followed by the appearance
154 of a target at the center of the visual display (straight ahead). After the monkey directed its gaze
155 toward its location within a surrounding invisible window (12° centered on the target) and for
156 a variable interval (ranging from 750 to 1500 ms by increments of 250 ms), the central target
157 moved centrifugally along a cardinal (horizontal and vertical meridians) or oblique axis with a
158 constant speed ($10^\circ/\text{s}$ during 1,200 ms, $20^\circ/\text{s}$ during 600 ms or $40^\circ/\text{s}$ during 300 ms), or with an
159 increasing (from 0 to $40^\circ/\text{s}$ during 600 ms) or decreasing speed (from 40 to $0^\circ/\text{s}$ during 600 ms).
160 The different types of target speed were tested in separate blocks of trials. Within each block,
161 the direction of target motion (cardinal or oblique) was pseudo-randomly selected (one out of
162 eight possible directions) in order to prevent the generation of anticipatory eye movements. The
163 monkeys' task was to track the target until the location where it disappeared at the end of the
164 trial. The fixation constraints for controlling the accuracy of eye movements were relaxed with
165 respect to requirements for obtaining their reward. Indeed, the monkeys had to direct their gaze
166 within a large invisible window around the moving target (12° centered on the moving target).
167 Otherwise, the trial was aborted and a new trial started. Our recordings show that these relaxed

168 constraints do not incite monkeys to perform inaccurate saccades (see Figs. 3, 5, 7 and 9 in
169 Bourrelly et al. 2018; see also Fleuriet and Goffart 2012; Quinet and Goffart 2015). Each
170 session (lasting 1 to 2 hours) was composed of different blocks of trials whose number
171 depended upon the monkey's motivation. Water-deprived in their home cage, the monkeys
172 obtained the water they need during daily sessions. A session ended when they stopped fixating
173 the central target for more than ten successive trials.

174 *Muscimol injection*

175 A thin cannula (beveled tip) was connected to a Hamilton syringe with polyethylene
176 tubing. We filled the inner volume with a saline solution of muscimol (2 $\mu\text{g}/\mu\text{l}$). The cannula
177 was lowered through the same guide tube used during the electrophysiological sessions and
178 aimed at the fastigial region where neurons emitted bursts during saccades. Small volumes (0.2–
179 1.1 μl) of muscimol were injected by small pulses over a time interval of approximately 15
180 minutes. The injected volume was checked by the displacement of a meniscus of air in the
181 tubing (1 mm corresponding to 0.1 μl). Before starting the recording of eye movements toward
182 a moving target, saccades toward static targets were recorded for approximately 15-30 minutes
183 in order to complete a companion study (Goffart et al. 2005, 2017; Quinet and Goffart 2016).
184 During the muscimol sessions, the blocks that tested the tracking of accelerating or decelerating
185 targets were always the last ones.

186 *Data analysis*

187 The results presented in this paper concern the data obtained before and after ten
188 unilateral muscimol injections performed in the cFN of two monkeys (6 injections in monkey
189 A, 4 in monkey Bi). For each experiment, the performance after muscimol injection was
190 compared with that recorded during the 3-4 preceding control daily sessions. No noticeable
191 difference was observed between the responses collected during the pre-injection sessions, so

192 movements were pooled together to include some day-to-day variability in our control dataset.
193 For each monkey, we injected muscimol into the left cFN in half of the experiments and in the
194 right cFN in the others. All data were digitized on-line and analyzed off-line using a custom-
195 made software program that detected the onset and offset of the horizontal and vertical
196 components of saccades on the basis of a velocity threshold ($30^\circ/\text{s}$). The results of this automatic
197 detection were checked by inspecting each trial individually, and were adjusted manually when
198 necessary. The present study describes the effect of unilateral cFN inactivation on the
199 interceptive saccades made in response to the target when it moved along the vertical meridian.
200 The effects of fastigial inactivation on movements toward the horizontally moving target were
201 thoroughly described elsewhere (Bourrelly et al. 2018a, b). The interceptive saccade
202 corresponds to the first saccade made from a static target toward the target after the onset of its
203 motion. To make sure that the interceptive saccade was not triggered prematurely, those with
204 latency < 80 ms were excluded from analysis (0.3% of the total number of trials). The Statistica
205 software (Statsoft) was used for statistical analyses and figure illustrations. Statistical
206 significance threshold was set to P-value < 0.05 . Because the size of deficits could differ
207 between different injections, the mean values of the pre- and post-injection movements were
208 compared with the non-parametric Wilcoxon test (for paired comparison). Thus, our main
209 conclusions are based on the systematic effects that were revealed by this overall comparison
210 across different experiments. The correlations between different behavioral measurements were
211 evaluated with the (parametric) Bravais-Pearson test whereas the correlation between a
212 behavioral parameters and the target speed was evaluated with the non-parametric Spearman
213 test.

214 **Results**

215 **Figure 1 approximately here**

216 Figure 1 illustrates with a few selected trials how a unilateral injection of muscimol in the cFN
217 affects the eye movements made in response to a centrifugal target moving at a constant speed
218 ($20^\circ/\text{s}$) along the vertical meridian. The time course of the horizontal (top row) and vertical
219 (bottom row) components is shown for movements produced before (gray) and after muscimol
220 injection (black) in the left (A and B: experiments A2 and A3 in monkey A) or right cFN (C:
221 experiment Bi9 in monkey Bi). As described elsewhere (Guerrasio et al. 2010), inactivation of
222 cFN caused a fixation offset toward the injected side. Most starting eye positions were shifted
223 to the right after muscimol injection in the right cFN (see black arrow in C) and to the left after
224 muscimol injection in the left cFN (black arrow in A). The ipsilesional offset was not observed
225 on every trial. We show examples (recorded during the experiments A2 and A3) in which the
226 saccades were initiated from positions near the vertical meridian (horizontal position values
227 close to zero in the upper graphs) but below the horizontal meridian (negative values of vertical
228 position in the lower graphs). In addition to altering gaze direction during fixation, unilateral
229 cFN inactivation also perturbed vertical saccades. Their trajectory was deviated horizontally
230 toward the injected side, regardless of whether the target moved upward or downward. In the
231 following paragraphs, after describing the velocity of their vertical component, we describe the
232 ipsipulsion that alters the trajectory of vertical saccades.

233 **Figure 2 approximately here**

234 As for horizontal saccades (see Fig. 2 in Bourrelly et al. 2018a), muscimol injection in
235 the cFN barely affected the vertical velocity of saccades. Figure 2 illustrates the vertical
236 amplitude-peak velocity relationship for four different experiments (two per monkey; A and B:
237 experiments A2 and A3 in monkey A; C and D: Bi7 and Bi8 in monkey Bi). The peak velocity

238 values are plotted for all upward and downward saccades (positive and negative amplitude
239 values, respectively) made in response to the different target speeds. When we consider
240 saccades of comparable vertical amplitude, we can see that the peak velocity is similar between
241 the pre and post-injection movements.

242 **Figure 3 approximately here**

243 Figure 3 describes the landing position and time of interceptive saccades made toward
244 a target moving with a constant speed ($20^\circ/\text{s}$) along the vertical meridian (black: upward
245 motion, gray: downward). For three different experiments (A3 and Bi7: left cFN inactivation;
246 Bi9: right cFN inactivation), the vertical (top row) and horizontal (bottom row) landing
247 positions are plotted as a function of their times relative to target motion onset. During the
248 control sessions (open squares), the vertical landing position increased as the landing time
249 increased, and the saccades were directed toward locations close to the physical target
250 (represented by the dashed lines). After muscimol injection (filled squares), the vertical landing
251 positions still increased as the landing time increased, regardless of the motion direction. The
252 overlap between pre- and post-injection data points indicates that unilateral cFN inactivation
253 did not noticeably affect the vertical component of interceptive saccades. Similar findings were
254 found with respect to saccades toward a static target (Goffart et al. 2004). By contrast, the
255 horizontal landing positions changed after muscimol injection. While they were scattered along
256 the vertical meridian (position values close to zero) during the control sessions, their
257 distribution was shifted toward the injected side after muscimol injection (to the left in
258 experiments A3 and Bi7, to the right in experiment Bi9). This effect is rather small in
259 experiment A3 (B: mean \pm standard deviation values changing from $-0.1 \pm 0.3^\circ$ to $-0.5 \pm 0.4^\circ$
260 after muscimol injection), but the change of horizontal position was much larger in experiments
261 Bi7 (D: from $0.0 \pm 0.3^\circ$ to $-3.5 \pm 1.6^\circ$), with Bi9 displaying intermediate values (F: from $0.3 \pm$
262 0.4° to $2.0 \pm 0.7^\circ$). Regardless of whether the target moved upward (black symbols) or

263 downward (gray symbols), the horizontal landing position was always shifted toward the
264 injected side. The size of the ipsipulsion was, in some cases, relatively constant (as in B) or
265 increased with the landing time (as in D). It is worth noting that the hypermetria of ipsilesional
266 horizontal saccades was relatively small during experiment A3 whereas it was larger during
267 experiments Bi7 and Bi9 (see Figures 7 and 10 in Bourrelly et al. 2018a). In summary, an
268 ipsilesional deviation was observed in the trajectory of vertical saccades during cFN
269 inactivation. The magnitude of the ipsipulsion varied between experiments, but as we will show,
270 it is correlated to the magnitude of the dysmetria that impairs the horizontal saccades.

271 To quantify the accuracy of vertical saccades, we calculated for each component the
272 ratio of landing position to landing time. This parameter (called position/time landing)
273 characterizes both spatial *and* temporal aspects of saccades made toward a moving target
274 (Bourrelly et al. 2018a). When we consider saccades toward a target moving along the vertical
275 meridian, the values of vertical position/time landing are expected to be close to the target speed
276 if gaze lands next to the target location. A ratio larger than the target speed indicates an
277 overshoot (too large amplitude) whereas a smaller value means an undershoot (too small
278 amplitude). Concerning the horizontal component, if gaze lands close to the target, its value is
279 expected to be close to zero because the target does not move horizontally. We will use the
280 convention that a positive horizontal ratio indicates an ipsilesional deviation whereas a negative
281 value is the signature of a contralesional deviation.

282 **Figure 4 approximately here**

283 Figure 4 shows the average vertical position/time landing relationships for each monkey
284 and each experiment in which the target moved at constant speed. During the control sessions,
285 the values were close to the target speed (11.2 ± 1.3 , 21.9 ± 2.0 and 38.9 ± 4.6 °/s for the 10, 20
286 and 40 °/s targets, respectively). After muscimol injection, these ratios were larger ($12.3 \pm$

287 3.8°/s, $24.3 \pm 4.0^\circ/\text{s}$ and $44.2 \pm 6.3^\circ/\text{s}$ for the 10, 20 and 40 °/s targets, respectively) (Fig. 4A).
288 This increase was small but statistically significant (Wilcoxon test, all P values < 0.05). A
289 stronger affect was observed in the horizontal component of vertical saccades. Figure 4B shows
290 the average horizontal position/time landings for each tested constant speed, in each experiment
291 and both monkeys. After muscimol injection, the horizontal position/time landings increased
292 from $0.0 \pm 0.7^\circ/\text{s}$ (range: $-1.1 - 1.6^\circ/\text{s}$) to $5.4 \pm 3.6^\circ/\text{s}$ (range: $0.8 - 12.1^\circ/\text{s}$) when the target
293 speed was 10°/s, from $0.0 \pm 1.1^\circ/\text{s}$ (range: $-2.6 - 2.9^\circ/\text{s}$) to $8.0 \pm 4.9^\circ/\text{s}$ (range: $1.8 - 18.6^\circ/\text{s}$)
294 with the 20°/s target and from $-0.2 \pm 1.6^\circ/\text{s}$ (range: $-2.5 - 2.9^\circ/\text{s}$) to $12.0 \pm 7.6^\circ/\text{s}$ (range: $3.1 -$
295 $24.2^\circ/\text{s}$) with the 40°/s target. The ranges of mean values and the examination of data points in
296 Fig 4B indicate more variability after muscimol injection than before (see the scattering toward
297 more positive values; note also the different scales for the x and y axes). During the control
298 sessions, the average horizontal position/time landings were close to zero (grand averages =
299 0.0, 0.0 and $-0.2^\circ/\text{s}$ for the 10, 20 and 40°/s target, respectively; all monkeys considered). After
300 muscimol injection, the values were larger and also increased with target speed (5.4, 8.0 and
301 $12.0^\circ/\text{s}$ for the 10, 20 and 40°/s target, respectively). Figure 4C compares the average horizontal
302 position/time landing between saccades toward the 20°/s target and saccades to the 10°/s (gray
303 symbols) and 40°/s (black symbols) targets. The values with the 10°/s target were smaller than
304 the values with the 20°/s target (gray symbols are situated below the diagonal line of equality)
305 whereas the values with the 40°/s target were larger than those obtained with the 20°/s target
306 (almost all black symbols above the diagonal line). Thus, within the same experiment, the size
307 of the ipsipulsion was larger during saccades to the fastest target than during saccades to the
308 slowest ones. Moreover, the injections which led to the larger horizontal errors with the 20°/s
309 target were those caused the bigger changes with the other speeds. Statistically significant
310 correlations were indeed found between the average horizontal position/time landing values
311 calculated with the 20°/s and 10°/s targets (Bravais-Pearson correlation coefficient $R = 0.94$, P

312 < 0.05) as well as between the mean values obtained with the 20°/s and 40°/s targets ($R(x,y) =$
313 0.93, $P < 0.05$).

314 **Figure 5 approximately here**

315 In our previous report, we documented the dysmetria of horizontal interceptive saccades
316 after cFN inactivation: ipsilesional saccades are hypermetric whereas contralesional saccades
317 are hypometric (Bourrelly et al. 2018a). Like the dysmetria that affects horizontal saccades
318 toward a static target (Goffart et al. 2004, in preparation), the sizes of the ipsilesional and
319 contralesional dysmetria are unrelated. However, it is known that the cFN projects to the region
320 in the contralateral medullary reticular formation (medRF) where premotor inhibitory burst
321 neurons (IBNs) are located (Noda et al. 1990) and that these neurons, in addition to firing a
322 burst during horizontal saccades, also fire during vertical saccades (Scudder et al. 1988; van
323 Gisbergen et al. 1981). Because of this involvement of IBNs in horizontal and vertical saccades,
324 it is quite reasonable to consider that a common dysfunction causes the ipsipulsion of vertical
325 saccades and the dysmetria of horizontal saccades (Goffart et al. 2004). Therefore, we tested
326 the relation between these two disorders and found a significant correlation between the average
327 horizontal position/time landings of ipsilesional horizontal saccades and vertical saccades
328 toward the 10°/s ($R = 0.77$, $P < 0.05$), 20°/s ($R = 0.62$, $P < 0.05$) and 40°/s ($R = 0.81$, $P < 0.05$)
329 targets (Fig. 5A). When the correlation was instead tested between the horizontal position/time
330 landings of contralesional horizontal saccades and vertical saccades, the coefficients were
331 smaller and negative. Furthermore, the correlation did not reach statistical significance when
332 the target moved at 10°/s ($R = -0.41$, $P > 0.05$) and 40°/s ($R = -0.13$, $P > 0.05$). A significant
333 correlation was found only with the 20°/s target ($R = -0.47$, $P < 0.05$) (Fig. 5B). Then, for each
334 experiment, we subtracted the average contralesional position/time landing from the
335 ipsilesional position/time landing, the resulting difference (hereafter called net bilateral effect
336 on horizontal saccades) characterizing the dysmetria of saccades made toward a target moving

337 horizontally (leftward or rightward). In this case, we found significant correlations between the
338 horizontal position/time landings of vertical saccades and the net bilateral effect on horizontal
339 saccades (Fig. 5C) that were stronger than those obtained with ipsilesional horizontal saccades
340 ($10^\circ/\text{s}$ target: $R = 0.91$ versus 0.77 ; $20^\circ/\text{s}$ $R = 0.81$ versus 0.62 ; $40^\circ/\text{s}$: $R = 0.90$ versus 0.81).

341 In summary, after muscimol injection in the cFN, all vertical saccades made toward a
342 target moving at a constant speed along the vertical meridian were deviated horizontally toward
343 the injected side. Their vertical components were slightly affected but not as dramatically as
344 the horizontal component. The size of the ipsipulsion differed between experiments and the
345 average horizontal position/time landing increased with the target speed. Moreover, the
346 ipsipulsion is correlated with the dysmetria that impaired the horizontal (ipsilesional and
347 contralesional) saccades.

348 **Figure 6 approximately here**

349 In the figure 4C, we showed that the ipsipulsion of vertical saccades depends upon the
350 target speed. To further explore this dependence, we tested saccades toward a target that moved
351 with continuous acceleration or deceleration. If the ipsipulsion depends on target speed, the
352 horizontal landing position should increase with later landing times when the target accelerates
353 but decrease or stagnate when it decelerates. Figure 6 describes the horizontal landing position
354 and time of saccades to a target moving with an increasing (top row) and decreasing speed
355 (bottom row) for three experiments (A3: left column; Bi8: middle and Bi9: right). During the
356 control sessions (open squares), the saccades landed on locations situated along the vertical
357 meridian (open symbols are close to the line of zero horizontal position) whereas after muscimol
358 injection (filled squares), they landed on locations which were shifted toward the injected side
359 (see negative position values in experiments A3 and Bi8 and positive values in experiment Bi9).
360 For these three experiments, the ipsipulsion of vertical saccades did not depend on the

361 instantaneous speed of the target. Statistically significant correlations were found in only two
362 experiments: A6 (positive correlation $R = 0.54$, injection in the right cFN) and A2 (negative
363 correlation $R = -0.35$, left cFN). For the other experiments, no correlation was found between
364 the horizontal landing position and the landing time when the target accelerated (R values
365 ranged from -0.25 to 0.19 , P -values > 0.05). Concerning the saccades toward a decelerating
366 target, no statistically significant correlation was found between the horizontal landing position
367 and the landing time (R values ranged from -0.42 to 0.34 , P -values > 0.05). In summary, we
368 found no evidence suggesting that the ipsipulsion depends on the instantaneous target speed:
369 the horizontal landing position neither increased with later landing times when the target
370 accelerated nor decreased when it decelerated.

371 **Figure 7 approximately here**

372 Fig. 7 documents the mean values of vertical (A) and horizontal (B) position/time
373 landing of saccades toward the accelerating (gray symbols) and decelerating (black symbols)
374 targets, before and after muscimol injection, as a summary of our results. The vertical
375 position/time landing of saccades was changed after muscimol injection, more with the
376 decelerating target than with the accelerating one (Fig. 7A). With the accelerating target, the
377 pre- and post-injection mean values of vertical position/time landing were not significantly
378 different (Wilcoxon test, $P = 0.47$) whereas with the decelerating target, the post-injection
379 values were significantly different from pre-injection values (16% average increase, $P < 0.05$).
380 Regarding the horizontal position/time landing (Fig. 7B), it increased from $0.1 \pm 0.7^\circ/s$ (range:
381 $-0.8 - 1.9^\circ/s$) to $5.0 \pm 2.9^\circ/s$ (range: $0.8 - 9.5^\circ/s$) after muscimol injection with the accelerating
382 target and from $0.0 \pm 1.8^\circ/s$ (range: $-3.6 - 3.4^\circ/s$) to $11.6 \pm 5.9^\circ/s$ (range: $2.6 - 20.1^\circ/s$) with the
383 decelerating target. In both groups of saccades, the changes were statistically significant ($P <$
384 0.05). Like saccades toward a target moving with a constant speed, the mean values of
385 horizontal landing position were also variable between the different muscimol injections (see

386 range values reported above and the scatter of post-lesion data points in Fig. 7B). Finally, the
387 injections which led to the larger horizontal position/time landings with the 20°/s moving target
388 were those which led to the bigger changes with the accelerating and decelerating targets (Fig.
389 7C). Statistically significant correlations were indeed found between the horizontal
390 position/time landings of saccades toward the 20°/s and those directed toward the accelerating
391 (Bravais-Pearson correlation coefficient $R(x,y) = 0.86$, $P < 0.05$) or decelerating target ($R(x,y)$
392 $= 0.90$ $P < 0.05$). In summary, all vertical saccades toward a target moving with a changing
393 speed were shifted horizontally after muscimol injection in the cFN. Like saccades toward a
394 target moving at a constant speed, the amplitude of their vertical component was slightly
395 increased after muscimol inactivation. Their horizontal component was biased toward the
396 injected side with a magnitude which differed between experiments. The ipsipulsion was larger
397 for saccades aimed toward a fast target than toward a slow target. It was also smaller when the
398 target accelerated than when it decelerated.

399 As for saccades to a target moving horizontally, the larger deficit with fast targets can
400 result from the fact that at identical landing times, a fast target is more eccentric than a slow
401 one. The dependency of the ipsipulsion upon the target speed can result from the fact that a
402 larger amplitude was required to intercept the target when it moves fast. Studies of vertical
403 saccades toward a static target do indeed show that after cFN inactivation, the ipsipulsion
404 increases with more eccentric targets (Goffart et al. 2004; Iwamoto and Yoshida 2002; Quinet
405 and Goffart 2007). However, increasing target eccentricity enhances both the amplitude and
406 duration of saccades for larger saccades that last longer. It is not known which of these
407 parameters affect more the magnitude of ipsipulsion. Therefore, we tested the correlation
408 between the horizontal landing position and saccade duration for each post-injection session.
409 The parameters of the equations fitting the relation between the horizontal landing position and
410 the saccade duration after muscimol injection are documented for all the experiments (upward

411 and downward movements pooled together) in table 1 (constant speeds) and table 2 (changing
412 speeds). The correlation was statistically significant in 13 out of 44 test sessions (corresponding
413 to 30% of cases) with coefficients of correlation ranging from 0.37 to 0.72. When we instead
414 considered the relation between the horizontal landing position and vertical saccade amplitude,
415 statistically significant correlations were found in 30 out of 44 experiments (corresponding to
416 68% of the post-injection sessions), with coefficients of correlation ranging from 0.38 to 0.81.
417 The parameters of the equations fitting the relation between the horizontal landing position and
418 the vertical saccade amplitude after muscimol injection are documented for all the experiments
419 (upward and downward movements pooled together) in table 1 (target moving at a constant
420 speed) and table 2 (accelerating and decelerating targets). Altogether, these results suggest that
421 it is more likely that the ipsipulsion increased because saccades had larger amplitudes than
422 because they lasted longer.

423 **Figure 8 approximately here**

424 To illustrate this correlation between the vertical amplitude of saccades and the
425 ipsipulsion, Fig. 8 plots the horizontal landing position as a function of vertical saccade
426 amplitude before and after muscimol injection. Both upward and downward saccades were
427 included (the amplitude of downward saccades was multiplied by -1). The relations are shown
428 for four injections made in the left cFN of monkey A (experiments A2 and A3, top row) and Bi
429 (experiments Bi7 and Bi8, bottom) for saccades to targets moving with a constant speed (light
430 gray, dark gray and black symbols correspond to the 10, 20 and 40°/s target speeds,
431 respectively). Negative values of horizontal eye position indicate that the saccades were
432 deviated toward the left (inactivated side). Thus, we can see that while the target speed increases
433 from 10 to 40°/s (symbols with different shades of grey), the horizontal landing position and
434 the vertical saccade amplitude increased. During experiment A2 (Fig. 8A), as the target speed
435 increased, the horizontal landing position changed from $-0.3 \pm 0.3^\circ$ (10°/s) to $-0.7 \pm 0.5^\circ$ (20°/s)

436 and $-1.4 \pm 0.8^\circ$ ($40^\circ/\text{s}$), while the vertical amplitude increased from $2.8 \pm 0.6^\circ$ ($10^\circ/\text{s}$) to $5.1 \pm$
437 1.1° ($20^\circ/\text{s}$) and $10.2 \pm 1.9^\circ$ ($40^\circ/\text{s}$). Likewise, during experiment A3 (Fig. 8B), the horizontal
438 landing position increased from $-0.3 \pm 0.3^\circ$ to $-0.5 \pm 0.4^\circ$ and $-1.3 \pm 0.6^\circ$ while the vertical
439 amplitude increased from $2.7 \pm 0.6^\circ$ to $5.1 \pm 1.1^\circ$ and $10.5 \pm 1.1^\circ$ (values for the 10, 20 and
440 $40^\circ/\text{s}$ target speed, respectively). The same relationship was found in monkey Bi. During
441 experiment Bi7 (Fig. 8C), the horizontal landing position increased from $-2.4 \pm 0.7^\circ$ to $-3.4 \pm$
442 1.6° and $-4.3 \pm 1.1^\circ$ and the vertical amplitude from $2.2 \pm 0.7^\circ$ to $5.1 \pm 1.2^\circ$ and $9.0 \pm 1.3^\circ$.
443 Finally, during experiment Bi8 (Fig. 8D), the horizontal landing position increased from $-2.0 \pm$
444 0.7° ($10^\circ/\text{s}$) to $-2.8 \pm 0.8^\circ$ ($20^\circ/\text{s}$) to $-3.7 \pm 1.0^\circ$ ($40^\circ/\text{s}$), while the vertical amplitude increased
445 from $2.2 \pm 0.6^\circ$ to $5.0 \pm 1.6^\circ$ and $9.1 \pm 1.1^\circ$. A relation was observed between the horizontal
446 landing position and the vertical amplitude of saccades. Each inset graph plotted in the right
447 part of the panels of Figure 8 shows an overlap of data points corresponding to saccades to a
448 target moving at constant speed (gray symbols) and to an accelerating or decelerating target
449 (black symbols). In summary, after cFN inactivation, the landing position of vertical saccades
450 was deviated toward the injected side by an amount that varied between experiments and that
451 was larger when the target moved quickly than when it moved slowly. The dependency of the
452 ipsipulsion upon the target speed indicates that the saccade oculomotor system has access to
453 different signals when the target moves at different speeds. However, the use of accelerating
454 and decelerating target enabled us to exclude a dependency upon the instantaneous speed of the
455 target. Further analyses revealed that the ipsipulsion was more frequently correlated with the
456 vertical amplitude of saccades rather than with their duration.

457 **Discussion**

458 This study is the first to describe the consequences of unilateral pharmacological
459 inactivation of cFN on the generation of vertical saccades toward a moving target. As for the
460 saccades toward a static target, interceptive saccades exhibit a horizontal deviation of their
461 trajectory toward the lesioned side (ipsipulsion; Figs. 3, 4B and 7B) whereas the vertical
462 component is barely affected (Figs. 3, 4A and 7A). The magnitude of the ipsipulsion is larger
463 for fast targets than for slowly moving targets (Fig. 4C) but the use of accelerating and
464 decelerating targets indicates that this relation is due less to the instantaneous target speed (Fig.
465 6) than to the saccade size. Indeed, like saccades toward a static target, the ipsipulsion increased
466 with the vertical amplitude of saccades (Fig. 8). Statistical analyses made across all sessions
467 indicate that the correlations between the ipsipulsion and the vertical amplitude were more
468 frequent than the correlations between the ipsipulsion and the duration. In the following, we
469 discuss the implications of our results after reminding the alternative viewpoint that we propose
470 to investigate the neurophysiology of saccades.

471

472 *Recasting the neurophysiology of saccades*

473 Saccades are engendered by an abrupt increase in the firing rate of motor neurons which
474 innervate the agonist muscles; a concomitant decrease happens in the neurons innervating the
475 antagonist muscles. Due to the highly damped nature of the oculomotor plant (Robinson 1964),
476 a braking action is not exerted upon the antagonist motor neurons to stop the saccade (Robinson
477 1970; Schiller 1970). While the agonist burst duration increases with the duration of saccades
478 and determines their size, a saturated firing rate leads to the firing frequency of the discharge
479 being poorly related to saccade speed (Fuchs and Luschei 1970; Robinson 1970; Schiller 1970).
480 For the generation of horizontal saccades, the burst causing the phasic contraction of the medial
481 rectus (and the saccade of the contralateral eye) originates in burst-tonic (internuclear) neurons

482 in the abducens nucleus while the burst causing the phasic contraction of the lateral rectus
483 (saccade of the ipsilateral eye) originates in abducens motoneurons. These bursts are caused by
484 excitatory burst neurons in the paramedian pontine reticular formation (Keller 1974; Luschei
485 and Fuchs 1972; Strassman et al. 1986a). It has been suggested that the discharge profile of
486 these neurons is a “replica of eye velocity” (Scudder et al. 2002). Their instantaneous firing rate
487 would be closely related with instantaneous eye velocity (Leigh and Zee 2006, page 126). Thus,
488 kinematic notions have been used to interpret the neuronal activity and to model the generation
489 of saccades. Beyond pragmatic reasons related to its simplicity, such a way of investigating the
490 neurophysiology of eye movements led to assume a correspondence between the discontinuous
491 emission of action potentials and the continuous changes in the orientation of the eyes. Yet, one
492 of the major founders of oculomotor physiology warned that “the models [...] do not contribute
493 much to the neurophysiology (or neurology) of eye movements and incur the danger of
494 suggesting that there actually are segregated portions of the nervous system which perform the
495 differentiation” (Robinson 1971, see also Becker 1995). Moreover, when we see that the firing
496 rate of premotor neurons does not exhibit the same time course as instantaneous eye velocity
497 (see Figs. 2 and 3 in Hu et al. 2007 and Fig. 5 in van Gisbergen et al. 1981), the
498 “neuronalization” of saccade velocity becomes quite questionable.

499 Each saccade is caused by changes in the firing rate of neurons distributed in many brain
500 regions. Its normal execution is altered when a perturbation affects the functioning of neurons
501 in the frontal cortex (Dias and Segraves 1999), mesencephalon (Aizawa and Wurtz 1998;
502 Sparks et al. 1990), pons (Kaneko and Fuchs 2006), cerebellum (Goffart et al. 2004; Kojima et
503 al. 2010) and reticular formation (Barton et al. 2003). Several studies reported on a relationship
504 between saccade velocity and the burst discharge of motoneurons (Sylvestre and Cullen 1999)
505 and premotor neurons (Cromer and Waitzman 2007; Cullen and Guitton 1997; King and Fuchs
506 1979). The correlation was recently extended to more central neurons in the superior colliculus

507 (SC) and the oculomotor vermis (Herzfeld et al. 2015; Smalianchuk et al. 2018). Consistent
508 with the crucial role of these two regions in continuously driving the saccades (Goffart et al.
509 2003; Goossens and van Opstal 2006), they proposed that the discharge of their neurons
510 “encodes” the instantaneous velocity. Beyond the fundamental concerns raised above and
511 elsewhere (Goffart et al. 2018; Goffart 2019), three major observations must be considered.
512 Firstly, the instantaneous firing rate of motoneurons is better fitted by a model factoring muscle
513 tension and its first derivative than by a model that uses eye position, velocity and acceleration
514 (Davis-Lopez de Carrizosa et al., 2011). Secondly, the instantaneous discharge of burst neurons
515 is clock-like and quasi-regular (Hu et al. 2007). Its time course is radically different from the
516 bell-shaped profile reported by studies which convolve each spike with a Gaussian kernel.
517 Thirdly, interposed between the saccade-related bursts of collicular and Purkinje cells on the
518 one hand, and the premotor bursts on the other hand, a population of neurons in the caudal
519 fastigial nuclei (cFN) emit spikes which have a strong impact on the trajectory of saccades
520 toward their landing position. Indeed, changes in cFN activity alter not only the endpoint of
521 saccades (Goffart et al. 2003; Noda et al. 1991) but also their trajectory (see Figs. 1 and 7 in
522 Goffart et al. 2004; Fig. 1 in Iwamoto and Yoshida 2002). The absence of relation between their
523 firing rate and saccade velocity (Fuchs et al. 1993; Helmchen et al. 1994; Ohtsuka and Noda
524 1991) draws into question the suggestion that the population discharge of Purkinje cells
525 “encodes” instantaneous saccade velocity (Herzfeld et al. 2015). When a correlation is found,
526 caution must be taken that it does not result from idiosyncrasy (all monkeys do not make the
527 same saccade amplitude with the same speed) or from unspecific factors like different levels of
528 motivation or arousal (Fuchs et al. 1993) as shown also in the deep superior colliculus (Ikeda
529 and Hikosaka 2007; Soetedjo et al. 2000). Finally, it is worth considering that if muscle tension
530 had been recorded (Davis-Lopez de Carrizosa et al., 2011; Gamlin and Miller; 2012;

531 Lennerstrand et al. 1993; Miller and Robins 1992) instead of eye position, different
532 neurophysiological processes would have been proposed.

533 **Figure 9 approximately here**

534 *How does bilateral fastigial activity influence the online steering of saccades?*

535 Numerous works show that the activity of cFN neurons plays a crucial role in the
536 brainstem control of saccade generation. Overlooking them runs the risk to make statements
537 which remain epiphenomenal; the causal relations between changes in firing rate and changes
538 in eye movements must be explained explicitly. Two major reasons led us to investigate this
539 influence on the steering of saccades made toward a target moving along the vertical meridian:
540 1) vertical saccades are deviated horizontally after unilateral cFN inactivation and 2) the same
541 etiology can account for this ipsipulsion and the dysmetria observed in horizontal saccades. In
542 the framework of negative feedback control in which internal estimate of current eye position
543 (or displacement) is compared to a desired eye position (or displacement) command (Robinson
544 1975; Sparks 1989; Becker 1995; Pola 2002), the horizontal bias could impair vertical saccades
545 in a cumulative manner as long as motor error is not zeroed and omnipause neurons do not
546 resume their activity (Goffart et al. 2004). Our results do not support this link between the
547 horizontal targeting error and the duration of vertical saccades because the magnitude of the
548 ipsipulsion was less frequently dependent upon duration than amplitude. An independence
549 between the dysmetria and duration of gaze shifts was already noticed in the head unrestrained
550 cat (see Figs. 5 and 6 in Goffart et al. 1998). Finally, because Soetedjo et al. (2000) reported no
551 change in the accuracy of saccades after muscimol injection in the nucleus raphe interpositus,
552 we are inclined to think that the dysmetria of saccades after cFN inactivation is not due to the
553 pause of OPNs (under the influence of the vertical burst generator). It seems more reasonable
554 to think that the ipsipulsion is actually caused by action potentials that abducens neurons emit
555 under the influence of unbalanced input from excitatory and inhibitory burst neurons.

556 The known physiology of the gaze circuitry indeed explains the ipsipulsion of vertical
557 saccades: if the activity of neurons in the left and right abducens nuclei is not balanced during
558 vertical saccades, there will be horizontal deviation of the eyes. The elevated speed and the
559 large magnitude of the ipsipulsion during head-unrestrained gaze shifts (Quinet and Goffart
560 2007) indicate that this imbalance is not caused by a reduced inhibition that IBNs in the
561 contralateral medullary reticular formation exert upon neurons in the abducens nucleus
562 ipsilateral to the inactivated cFN (synapses a and b in Fig. 9). An excitatory drive is required
563 and we hypothesize that it is conveyed by neurons in the opposite (unaffected) cFN (synapse
564 f). Transmitted by crossed projections (Noda et al. 1990), their spikes excite premotor burst
565 neurons in the pontomedullary reticular formation ipsilateral to the inactivated cFN, which in
566 turn activate motor and internuclear neurons in the ipsilateral abducens nucleus (synapses g and
567 h). This crossed excitatory influence upon premotor burst neurons is supported by the fact that
568 fastigial electrical stimulation evokes contralateral saccades (Cogdell et al. 1977; Noda et al.
569 1988; Quinet and Goffart 2015). It is also consistent with the contrapulsion of vertical saccades
570 when the oculomotor vermis is asymmetrically lesioned (Takagi et al. 1998) or inactivated with
571 muscimol (Nitta et al. 2007). This crossed fastigioreticular projection does not concern the
572 reticulospinal neurons that Takahashi et al. (2014) identified in the cat. Indeed, if it also exists
573 in the macaque, this fastigio-reticulospinal connection is likely involved in the postural tone of
574 the head because the head barely moves when the cFN is electrically stimulated (Quinet and
575 Goffart 2009). Also, during cFN inactivation in both the cat and monkey, the head exhibits an
576 ipsilesional deviation (Goffart and Pélisson 1998; Quinet and Goffart 2005). Furthermore, the
577 increase of ipsipulsion with saccade amplitude indicates that abducens neurons and excitatory
578 burst neurons (EBNs) fire more as the vertical amplitude increases. Although EBNs do not
579 normally fire during vertical saccades (Strassman et al. 1986a; Sparks et al. 2002) and unilateral
580 inactivation of their territory yields no ipsipulsion (Barton et al. 2003), it is possible that after

581 cFN inactivation, ipsilateral MNs, INs and EBNs abnormally fire during vertical saccades
582 because they are released from the inhibition exerted by burst neurons (IBNs) in the
583 contralateral reticular formation (synapses a, b and d; Cullen and Guitton 1997; Scudder et al.
584 1988; Strassman et al. 1986b). Those IBNs are silenced because of the suppression of their
585 fastigial drive (synapse i) by the muscimol injection, because also of the inhibition exerted by
586 IBNs located in the opposite side (synapse j) and recruited by neurons in the unaffected cFN
587 (synapse e). Scudder et al. (1988) indeed showed that IBNs fire more spikes as the size of
588 vertical saccades increases (see also van Gisbergen et al. 1981). Thus, when released from the
589 inhibitory influence of contralateral IBNs (synapses a and b), MNs and INs emit spikes that
590 deviate vertical saccades with a magnitude that increases with saccade size. The burst would be
591 triggered by excitatory input from EBNs or from other neurons innervating the abducens
592 nucleus (Langer et al. 1986; Ugolini et al. 2006).

593 According to the bilateral hypothesis, the activity of saccade-related fastigial neurons
594 influences the horizontal component of all saccades (vertical and/or horizontal). Ipsilesional
595 saccades overshoot horizontally their target because following cFN inactivation, the agonist
596 motor neurons receive a drive from excitatory burst neurons that exceeds the pre-lesional drive,
597 as it is no longer attenuated by spikes emitted by IBNs in the contralateral side. Indeed, these
598 IBNs not only lack their fastigial excitatory input but they are also inhibited by IBNs driven by
599 neurons in the unaffected cFN. Likewise, contralesional saccades prematurely stop for two
600 reasons: because the agonist motor neurons lack the drive they usually receive from EBNs (as
601 a result of suppressing their fastigial input) and because the opposite (unaffected) cFN excites
602 IBNs which in turn inhibit the agonist motor neurons. Thus, regardless of saccade direction, the
603 same bilateral mechanism (altered balance of excitatory and inhibitory input to the motor
604 neurons) explains the effects on the horizontal component of all saccades. This conclusion is
605 further supported when the results from the present study are synthesized with those reported

606 in Bourrelly et al. (2018a). Indeed, the net bilateral effect of inactivation on horizontal saccades
607 (calculated by subtracting the average contralesional position/time landing ratio from the
608 ipsilesional ratio) is strongly correlated with the horizontal position/time landing of vertical
609 saccades.

610

611 ***Conclusion***

612 Instead of reflecting the reduction of an internal signal encoding the horizontal distance
613 between gaze and target positions (or displacements), the horizontal component of saccades can
614 be viewed as the outcome of a process which restores, under bilateral fastigial control, an
615 equilibrium (symmetry) that has been broken by asymmetric descending input from cortical eye
616 fields and deep superior colliculus to the horizontal saccade generators. According to this
617 alternative theory, speed is not encoded in the discharge of neurons in the brainstem. Calculated
618 from eye position measurements, speed is the physical expression of an intrinsic process that
619 opposes mutually antagonist motor processes (Goffart et al. 2018; Goffart 2019). In the future,
620 more studies will have to clarify the cerebellar control of the vertical component of saccades
621 (see page 3333 in Quinet and Goffart 2015; Robinson 2000) and its coupling with the processes
622 controlling their horizontal component (Goffart et al. 2005).

623

624 **References**

- 625 Aizawa H, Wurtz RH. Reversible inactivation of monkey superior colliculus. I. Curvature of
626 saccadic trajectory. *J Neurophysiol* 79: 2082-2096, 1998. doi: [10.1152/jn.1998.79.4.2082](https://doi.org/10.1152/jn.1998.79.4.2082)
- 627 Barton EJ, Nelson JS, Gandhi NJ, Sparks DL. Effects of partial lidocaine inactivation of the
628 paramedian pontine reticular formation on saccades of macaques. *J Neurophysiol* 90: 372-
629 386, 2003. doi: [10.1152/jn.01041.2002](https://doi.org/10.1152/jn.01041.2002)
- 630 Becker W. Models of oculomotor function: An appraisal of the engineer's intrusion into
631 oculomotor physiology. *Studies Vis Inform Processing* 6: 23-46, 1995.
- 632 Bourrelly C, Quinet J, Cavanagh P, Goffart L. Learning the trajectory of a moving visual
633 target and evolution of its tracking in the monkey. *J Neurophysiol* 116: 2739–2751, 2016. doi:
634 [10.1152/jn.00519.2016](https://doi.org/10.1152/jn.00519.2016)
- 635 Bourrelly C, Quinet J, Goffart L. The caudal fastigial nucleus and the steering of saccades
636 toward a moving visual target. *J Neurophysiol* 120: 421–438, 2018a. doi:
637 [10.1152/jn.00141.2018](https://doi.org/10.1152/jn.00141.2018)
- 638 Bourrelly C, Quinet J, Goffart L. Pursuit disorder and saccade dysmetria after caudal fastigial
639 inactivation in the monkey. *J Neurophysiol* 120: 1640-1654, 2018b. doi:
640 [10.1152/jn.00278.2018](https://doi.org/10.1152/jn.00278.2018)
- 641 Bourrelly C, Quinet J, Goffart L. Unsupervised dynamic morphing of a spatiotemporal visual
642 event during its oculomotor tracking. *J Vision* 14: 492, 2014.
- 643 Buzunov E, Mueller A, Straube A, Robinson FR. When during horizontal saccades in monkey
644 does cerebellar output affect movement? *Brain Res* 1503: 33-42, 2013. doi:
645 [10.1016/j.brainres.2013.02.001](https://doi.org/10.1016/j.brainres.2013.02.001)
- 646 Cogdell B, Hassul M, Kimm J. Fastigial evoked eye movement and brain stem neuronal
647 behavior in the alert monkey. *Arch Otolaryngol* 103: 658-666, 1977. doi:
648 [10.1001/archotol.1977.00780280058008](https://doi.org/10.1001/archotol.1977.00780280058008)
- 649 Cromer JA, Waitzman DM. Comparison of saccade-associated neuronal activity in the
650 primate central mesencephalic and paramedian pontine reticular formations. *J Neurophysiol*
651 98: 835-850, 2007. doi: [10.1152/jn.00308.2007](https://doi.org/10.1152/jn.00308.2007)

652 Cullen KE, Guitton D. Analysis of primate IBN spike trains using system identification
653 techniques. I. Relationship to eye movement dynamics during head-fixed saccades. J
654 Neurophysiol 78: 3259-3282, 1997. doi : [10.1152/jn.1997.78.6.3259](https://doi.org/10.1152/jn.1997.78.6.3259)

655 Davis-López de Carrizosa MA, Morado-Díaz CJ, Miller JM, de la Cruz RR, Pastor ÁM. Dual
656 encoding of muscle tension and eye position by abducens motoneurons. J Neurosci 31: 2271-
657 2279, 2011. doi: [10.1523/JNEUROSCI.5416-10.2011](https://doi.org/10.1523/JNEUROSCI.5416-10.2011)

658 Dias EC, Segraves MA. Muscimol-induced inactivation of monkey frontal eye field: effects
659 on visually and memory-guided saccades. J Neurophysiol 81: 2191-2214, 1999. doi:
660 [10.1152/jn.1999.81.5.2191](https://doi.org/10.1152/jn.1999.81.5.2191)

661 Fuchs AF, Brettler S, Ling L. Head-free gaze shifts provide further insights into the role of the
662 medial cerebellum in the control of primate saccadic eye movements. J Neurophysiol 103:
663 2158–2173, 2010. doi: [10.1152/jn.91361.2008](https://doi.org/10.1152/jn.91361.2008)

664 Fuchs AF, Luschei ES. Firing patterns of abducens neurons of alert monkeys in relationship
665 to horizontal eye movement. J Neurophysiol 33: 382–392, 1970. doi:
666 [10.1152/jn.1970.33.3.382](https://doi.org/10.1152/jn.1970.33.3.382)

667 Fuchs AF, Kaneko CRS, Scudder CA. Brainstem control of saccadic eye movements. Ann
668 Rev Neurosci 8: 307-337, 1985. doi: [10.1146/annurev.ne.08.030185.001515](https://doi.org/10.1146/annurev.ne.08.030185.001515)

669 Fuchs AF, Robinson FR, Straube A. Role of the caudal fastigial nucleus in saccade
670 generation. I. Neuronal discharge pattern. J Neurophysiol 70: 1723-1740, 1993. doi:
671 [10.1152/jn.1993.70.5.1723](https://doi.org/10.1152/jn.1993.70.5.1723)

672 Gamlin, PD, Miller JM. Extraocular muscle motor units characterized by spike-triggered
673 averaging in alert monkey. J Neurosci Methods 204: 159-167, 2012. doi:
674 [10.1016/j.jneumeth.2011.11.012](https://doi.org/10.1016/j.jneumeth.2011.11.012)

675 Goffart L. Kinematics and the neurophysiological study of visually-guided eye movements.
676 Prog Brain Res 249:375-384, 2019. doi: [10.1016/bs.pbr.2019.03.027](https://doi.org/10.1016/bs.pbr.2019.03.027)

677 Goffart L, Péliesson D. Orienting gaze shifts during muscimol inactivation of caudal fastigial
678 nucleus in the cat. I. Gaze dysmetria. J Neurophysiol 79: 1942–1958, 1998.
679 doi:10.1152/jn.1998.79.4.1942

680 Goffart L, Pélisson D, Guillaume A. Orienting gaze shifts during muscimol inactivation of
681 caudal fastigial nucleus in the cat. II. Dynamics and eye-head coupling. *J Neurophysiol* 79:
682 1959-1976, 1998. doi: [10.1152/jn.1998.79.4.1959](https://doi.org/10.1152/jn.1998.79.4.1959)

683 Goffart L, Quinet J, Bourrelly C. Cerebellar control of saccades by the size of the active
684 population in the caudal fastigial nucleus (Abstract). 2017: 60.06, 2017. doi:

685 Goffart L, Bourrelly C, Quinton JC. Neurophysiology of visually-guided eye movements:
686 Critical review and alternative viewpoint. *J Neurophysiol* 120: 3234-3245, 2018. doi:
687 [10.1152/jn.00402.2018](https://doi.org/10.1152/jn.00402.2018)

688 Goffart L, Chen LL, Sparks DL. Saccade dysmetria during functional perturbation of the
689 caudal fastigial nucleus in the monkey. *Ann NY Acad Sci* 1004: 220-228, 2003. doi:
690 [10.1196/annals.1303.019](https://doi.org/10.1196/annals.1303.019)

691 Goffart L, Chen LL, Sparks DL. Deficits in saccades and fixation during muscimol
692 inactivation of the caudal fastigial nucleus in the rhesus monkey. *J Neurophysiol* 92: 3351-
693 3367, 2004. doi: [10.1152/jn.01199.2003](https://doi.org/10.1152/jn.01199.2003)

694 Goffart L, Koene A, Quinet J. Coupling between horizontal and vertical saccade generators
695 after muscimol injection in the monkey caudal fastigial nucleus. *Soc Neurosci Abstr* 475.2,
696 2005.

697 Goffart L, Quinet J, Bourrelly C. Cerebellar control of saccades by the size of the active
698 population in the caudal fastigial nucleus. S-5042-SfN, 2017c.

699 Goossens HH, Van Opstal AJ. Dynamic ensemble coding of saccades in the monkey superior
700 colliculus. *J Neurophysiol* 95: 2326–2341, 2006. doi: [10.1152/jn.00889.2005](https://doi.org/10.1152/jn.00889.2005)

701 Guerrasio L, Quinet J, Büttner U, Goffart L. Fastigial oculomotor region and the control of
702 foveation during fixation. *J Neurophysiol* 103: 1988-2001, 2010. doi: [10.1152/jn.00771.2009](https://doi.org/10.1152/jn.00771.2009)

703 Helmchen C, Straube A, Büttner U. Saccade-related activity in the fastigial oculomotor region
704 of the macaque monkey during spontaneous eye movements in light and darkness. *Exp Brain*
705 *Res* 98: 474–482, 1994. doi: [10.1007/BF00233984](https://doi.org/10.1007/BF00233984)

706 Hepp K, Henn V, Vilis T, Cohen B. Brainstem regions related to saccade generation. In: The
707 neurobiology of saccadic eye movements. RH Wurtz and ME Goldberg (eds), Elsevier, 1989,
708 pp 105-212.

709 Herzfeld DJ, Kojima Y, Soetedjo T, Shadmehr R. Encoding of action by the Purkinje cells of
710 the cerebellum. *Nature* 526: 439-442, 2015. doi: [10.1038/nature15693](https://doi.org/10.1038/nature15693)

711 Horn AK. The reticular formation. *Progr Brain Res* 151: 127-155, 2006. doi:

712 Hu X, Jiang H, Gu C, Li C, Sparks DL. Reliability of oculomotor command signals carried by
713 individual neurons. *Proc Nat Acad Sci* 104: 8137-8142, 2007. doi: [10.1073/pnas.0702799104](https://doi.org/10.1073/pnas.0702799104)

714 Ikeda T, Hikosaka O. Positive and negative modulation of motor response in primate superior
715 colliculus by reward expectation. *J Neurophysiol* 98: 3163-3170, 2007. doi:
716 [10.1152/jn.00975.2007](https://doi.org/10.1152/jn.00975.2007)

717 Iwamoto Y, Yoshida K. Saccadic dysmetria following inactivation of the primate fastigial
718 oculomotor region. *Neurosci Lett* 325: 211-215, 2002. doi: [10.1016/s0304-3940\(02\)00268-9](https://doi.org/10.1016/s0304-3940(02)00268-9)

719 Kaneko CR, Fuchs AF. Effect of pharmacological inactivation of nucleus reticularis tegmenti
720 pontis on saccadic eye movements in the monkey. *J Neurophysiol* 95: 3698-3711, 2006. doi:
721 [10.1152/jn.01292.2005](https://doi.org/10.1152/jn.01292.2005)

722 Keller EL. Participation of medial pontine reticular formation in eye movement generation in
723 monkey. *J Neurophysiol* 37: 316-332, 1974. doi: [10.1152/jn.1974.37.2.316](https://doi.org/10.1152/jn.1974.37.2.316)

724 King WM, Fuchs AF. Reticular control of vertical saccadic eye movements by mesencephalic
725 burst neurons. *J Neurophysiol* 42: 861-876, 1979. doi: [10.1152/jn.1979.42.3.861](https://doi.org/10.1152/jn.1979.42.3.861)

726 Kleine JF, Guan Y, Büttner U. Saccade-related neurons in the primate fastigial nucleus: what
727 do they encode? *J Neurophysiol* 90: 3137-3154, 2003. doi: [10.1152/jn.00021.2003](https://doi.org/10.1152/jn.00021.2003)

728 Kojima Y, Soetedjo R, Fuchs AF. Effects of GABA agonist and antagonist injections into the
729 oculomotor vermis on horizontal saccades. *Brain Res* 1366: 93-100, 2010. doi:
730 [10.1016/j.brainres.2010.10.027](https://doi.org/10.1016/j.brainres.2010.10.027)

731 Langer T, Kaneko CR, Scudder CA, Fuchs AF. Afferents to the abducens nucleus in the
732 monkey and cat. *J Comp Neurol* 245: 379-400, 1986. doi : [10.1002/cne.902450307](https://doi.org/10.1002/cne.902450307)

733 Leigh RJ, Zee DS. *The neurology of eye movements*. Oxford University Press, 2006.

734 Lennerstrand G, Tian S, Zhao TX. Force development and velocity of human saccadic eye
735 movements. I: Abduction and adduction. *Clinical vision sciences* 8: 295-305, 1993.

736 Luschei ES, Fuchs AF. Activity of brain stem neurons during eye movements of alert
737 monkeys. *J Neurophysiol* 35: 445-461, 1972. doi: [10.1152/jn.1972.35.4.445](https://doi.org/10.1152/jn.1972.35.4.445)

738 Miller JM, Robins D. Extraocular muscle forces in alert monkey. *Vision Res* 32: 1099-1113,
739 1992. doi: [10.1016/0042-6989\(92\)90010-g](https://doi.org/10.1016/0042-6989(92)90010-g)

740 Moschovakis AK, Scudder CA, Highstein SM. The microscopic anatomy and physiology of
741 the mammalian saccadic system. *Prog Neurobiol* 50: 133-254, 1996. doi: [10.1016/s0301-](https://doi.org/10.1016/s0301-0082(96)00034-2)
742 [0082\(96\)00034-2](https://doi.org/10.1016/s0301-0082(96)00034-2)

743 Nitta T, Akao T, Kurkin S, Fukushima K. Involvement of the cerebellar dorsal vermis in
744 vergence eye movements in monkeys. *Cereb Cortex* 18: 1042-1057, 2008. doi:
745 [10.1093/cercor/bhm143](https://doi.org/10.1093/cercor/bhm143)

746 Noda H, Murakami S, Warabi T. Effects of fastigial stimulation upon visually-directed
747 saccades in macaque monkeys. *Neurosci Res* 10(3):188-99, 1991. doi: [10.1016/0168-](https://doi.org/10.1016/0168-0102(91)90056-5)
748 [0102\(91\)90056-5](https://doi.org/10.1016/0168-0102(91)90056-5)

749 Noda H, Murakami S, Yamada J, Tamada J, Tamaki Y, Aso T. Saccadic eye movements
750 evoked by microstimulation of the fastigial nucleus of macaque monkeys. *J Neurophysiol* 60:
751 1036–1052, 1988. doi: [10.1152/jn.1988.60.3.1036](https://doi.org/10.1152/jn.1988.60.3.1036)

752 Noda H, Sugita S, Ikeda Y. Afferent and efferent connections of the oculomotor region of the
753 fastigial nucleus in the macaque monkey. *J Comp Neurol* 302: 330-348, 1990. doi:
754 [10.1002/cne.903020211](https://doi.org/10.1002/cne.903020211)

755 Ohtsuka K, Noda H. Saccadic burst neurons in the oculomotor region of the fastigial nucleus
756 of macaque monkeys. *J Neurophysiol* 65: 1422-1434, 1991. doi: [10.1152/jn.1991.65.6.1422](https://doi.org/10.1152/jn.1991.65.6.1422)

757 Optican LM. Sensorimotor transformation for visually guided saccades. *Ann NY Acad Sci*
758 1039: 132-148, 2005. doi: [10.1196/annals.1325.013](https://doi.org/10.1196/annals.1325.013)

759 Pola J. Models of the saccadic and smooth pursuit systems. In *Models of the visual system*, G.
760 K. Hung et al. (eds.), Springer, Boston, MA, 2002, pp. 385-429.

761 Quinet J, Goffart L. Saccade dysmetria in head unrestrained gaze shifts after muscimol
762 inactivation of the caudal fastigial nucleus in the monkey. *J Neurophysiol* 93: 2343–2349,
763 2005. doi: [10.1152/jn.00705.2004](https://doi.org/10.1152/jn.00705.2004)

764 Quinet J, Goffart L. Head unrestrained gaze shifts after muscimol injection in the caudal
765 fastigial nucleus of the monkey. *J Neurophysiol* 98: 3269-3283, 2007. doi:
766 [10.1152/jn.00741.2007](https://doi.org/10.1152/jn.00741.2007)

767 Quinet J, Goffart L. Electrical microstimulation of the fastigial oculomotor region in the head-
768 unrestrained monkey. *J Neurophysiol* 102: 320-336, 2009. doi: [10.1152/jn.90716.2008](https://doi.org/10.1152/jn.90716.2008)

769 Quinet J, Goffart L. Does the brain extrapolate the position of a transient moving target? *J*
770 *Neurosci* 35: 11780-11790, 2015a. doi: [10.1523/JNEUROSCI.1212-15.2015](https://doi.org/10.1523/JNEUROSCI.1212-15.2015)

771 Quinet J, Goffart L. Cerebellar control of saccade dynamics: contribution of the fastigial
772 oculomotor region. *J Neurophysiol* 113: 3323–3336, 2015b. doi: [10.1152/jn.01021.2014](https://doi.org/10.1152/jn.01021.2014)

773 Quinet J, Goffart L. Bilateral fastigial control of the horizontal amplitude of saccades:
774 evidence from studying the orthogonal component after unilateral inactivation. *Soc Neurosc*
775 *Abstr* 55.03, 2016.

776 Robinson DA. The mechanics of human saccadic eye movement. *J Physiol* 174: 245-264,
777 1964. doi: [10.1113/jphysiol.1964.sp007485](https://doi.org/10.1113/jphysiol.1964.sp007485)

778 Robinson DA. Oculomotor unit behavior in the monkey. *J Neurophysiol* 33: 393-403,1970.
779 doi: [10.1152/jn.1970.33.3.393](https://doi.org/10.1152/jn.1970.33.3.393)

780 Robinson DA. Models of oculomotor neural organization. In: *The control of eye movements*,
781 P. Bach-Y-Rita, C Collins and J.E. Hyde (eds), 1971, pp 519-538.

782 Robinson DA. A quantitative analysis of extraocular muscle cooperation and squint.
783 Investigative Ophthalmology & Visual Sci. 14: 801-825, 1975.

784 Robinson FR. Role of the cerebellar posterior interpositus nucleus in saccades I. Effect of
785 temporary lesions. J Neurophysiol 84: 1289-1302, 2000. doi: [10.1152/jn.2000.84.3.1289](https://doi.org/10.1152/jn.2000.84.3.1289)

786 Robinson FR, Fuchs AF. The role of the cerebellum in voluntary eye movements. Annu Rev
787 Neurosci 24: 981-1004, 2001. doi: [10.1146/annurev.neuro.24.1.981](https://doi.org/10.1146/annurev.neuro.24.1.981)

788 Robinson FR, Straube A, Fuchs AF. Role of the caudal fastigial nucleus in saccade
789 generation. II. Effects of muscimol inactivation. J Neurophysiol 70: 1741–1758, 1993. doi:
790 [10.1152/jn.1993.70.5.1741](https://doi.org/10.1152/jn.1993.70.5.1741)

791 Schiller PH. The discharge characteristics of single units in the oculomotor and abducens
792 nuclei of the unanesthetized monkey. Exp Brain Res 10: 347-362, 1970. doi:
793 [10.1007/BF02324764](https://doi.org/10.1007/BF02324764)

794 Scudder CA, Fuchs AF, Langer TP. Characteristics and functional identification of saccadic
795 inhibitory burst neurons. J Neurophysiol 59: 1430-1454, 1988. doi:
796 [10.1152/jn.1988.59.5.1430](https://doi.org/10.1152/jn.1988.59.5.1430)

797 Scudder CA, Kaneko CS, Fuchs AF. The brainstem burst generator for saccadic eye
798 movements: a modern synthesis. Exp Brain Res 142: 439-462, 2002. doi: [10.1007/s00221-](https://doi.org/10.1007/s00221-001-0912-9)
799 [001-0912-9](https://doi.org/10.1007/s00221-001-0912-9)

800 Smalianchuk I, Jagadisan UK, Gandhi NJ. Instantaneous midbrain control of saccade velocity.
801 J. Neurosci. 38: 10156-10167, 2018. doi: [10.1523/JNEUROSCI.0962-18.2018](https://doi.org/10.1523/JNEUROSCI.0962-18.2018)

802 Soetedjo R, Kaneko CR, Fuchs AF. Evidence that the superior colliculus participates in the
803 feedback control of saccadic eye movements. J Neurophysiol 87: 679–695, 2000. doi:
804 [10.1152/jn.00886.2000](https://doi.org/10.1152/jn.00886.2000)

805 Sparks DL. The neural encoding of the location of targets for saccadic eye movements. J Exp
806 Biol 146: 195-207, 1989. doi:

807 Sparks DL, Barton EJ. Neural control of saccadic eye movements. Curr Opin Neurobiol 3:
808 966–972, 1993. doi: [10.1016/0959-4388\(93\)90169-y](https://doi.org/10.1016/0959-4388(93)90169-y)

809 Sparks DL, Barton EJ, Gandhi NJ, Nelson J. Studies of the role of the paramedian pontine
810 reticular formation in the control of head-restrained and head-unrestrained gaze shifts. *Annals*
811 *NY Acad Sciences* 956: 85-98, 2002. doi: [10.1111/j.1749-6632.2002.tb02811.x](https://doi.org/10.1111/j.1749-6632.2002.tb02811.x)

812 Sparks DL, Lee C, Rohrer WH. Population coding of the direction, amplitude, and velocity of
813 saccadic eye movements by neurons in the superior colliculus. *Cold Spring Harb Symp Quant*
814 *Biol* 55: 805–811, 1990. doi: [10.1101/sqb.1990.055.01.075](https://doi.org/10.1101/sqb.1990.055.01.075)

815 Strassman A, Highstein SM, McGrea RA. Anatomy and physiology of saccadic burst neurons
816 in the alert squirrel monkey. I. Excitatory burst neurons. *J Comp Neurol* 249: 337–357, 1986a.
817 doi: [10.1002/cne.902490303](https://doi.org/10.1002/cne.902490303)

818 Strassman A, Highstein SM, McCrea RA. Anatomy and physiology of saccadic burst neurons
819 in the alert squirrel monkey. II. Inhibitory burst neurons. *J Comp Neurol* 249: 358–380,
820 1986b. doi: [10.1002/cne.902490304](https://doi.org/10.1002/cne.902490304)

821 Sylvestre PA and Cullen KE. Quantitative analysis of abducens neuron discharge dynamics
822 during saccadic and slow eye movements. *J Neurophysiol* 82: 2612-2632, 1999. doi:
823 [10.1152/jn.1999.82.5.2612](https://doi.org/10.1152/jn.1999.82.5.2612)

824 Takagi M, Zee DS, Tamargo RJ. Effects of lesions of the oculomotor vermis on eye
825 movements in primate: saccades. *J Neurophysiol* 80: 1911-1931, 1998. doi:
826 [10.1152/jn.1998.80.4.1911](https://doi.org/10.1152/jn.1998.80.4.1911)

827 Takahashi M, Sugiuchi Y, Shinoda Y. Convergent synaptic inputs from the caudal fastigial
828 nucleus and the superior colliculus onto pontine and pontomedullary reticulospinal neurons. *J*
829 *Neurophysiol* 111: 849–967, 2014. doi: [10.1152/jn.00634.2013](https://doi.org/10.1152/jn.00634.2013)

830 Ugolini G, Klam F, Doldan Dans M, Dubayle D, Brandi A-M, Büttner-Ennever J, Graf W.
831 Horizontal eye movement networks in primates as revealed by retrograde transneuronal
832 transfer of rabies virus: differences in monosynaptic input to "slow" and "fast" abducens
833 motoneurons. *J Comp Neurol* 20: 498: 762-785, 2006. [10.1002/cne.21092](https://doi.org/10.1002/cne.21092)

834 van Gisbergen JAM, Robinson DA, Gielen S. A quantitative analysis of generation of
835 saccadic eye movements by burst neurons. *J Neurophysiol* 45: 417-442, 1981. doi:
836 [10.1152/jn.1981.45.3.417](https://doi.org/10.1152/jn.1981.45.3.417)

837

838 **Legends of figures**

839 Fig. 1. Effect of unilateral muscimol injection in the caudal fastigial nucleus on tracking a visual
840 target moving along the vertical meridian. The time course of eye movements produced before
841 (gray) and after (black) unilateral muscimol injection in the cFN is shown for six different trials.
842 The eye position (horizontal: upper row; vertical: bottom row) is plotted as a function of time
843 after target motion onset. The target moved at the constant speed of 20°/s. The selected trials
844 were recorded during the experiments A2 (A, injection in left cFN) and A3 (B, left cFN) in
845 monkey A and the experiment Bi9 (C, injection in the right cFN) in monkey Bi.

846

847 Fig. 2. Amplitude-peak velocity relationship of the vertical component of interceptive saccades
848 toward a target moving along the vertical meridian. This relationship is shown for two
849 experiments made in each monkey (upper row: A2 and A3 in monkey A; lower row: Bi7 and
850 Bi8 in monkey Bi), before (gray symbols) and after muscimol injection in the left cFN (black
851 symbols). The different symbols indicate the different target speeds (●: 10°/s, ■: 20°/s, *: 40°/s,
852 ▲: accelerating target, ◆: decelerating target). The number of observations are reported in the
853 tables 1 and 2.

854

855 Fig. 3. Landing position and time of saccades toward a target moving at constant speed along
856 the vertical meridian. The vertical (top row) and horizontal (bottom row) landing positions are
857 plotted as a function of the time after target motion onset when the target moved vertically at
858 20°/s. Data from before (open symbols) and after (solid symbols) muscimol injection is plotted.
859 Black and gray symbols correspond to the upward and downward moving target, respectively.
860 For each monkey, the effects of muscimol injection in the left or right cFN are documented (left
861 cFN: experiments A3 and Bi7: A-D, right cFN: experiment Bi9: E-F). The dashed line
862 corresponds to the target position.

863

864 Fig. 4. Position/time landing of saccades toward a target moving at constant speed along the
865 vertical meridian. The average values of the vertical (panel A) and horizontal (panel B)
866 components are plotted for the pre- and post-injection sessions of each experiment (square
867 symbols: monkey A; circle symbols: monkey Bi). The light gray, dark gray and black symbols

868 correspond to the 10, 20 and 40°/s target speeds, respectively. Open and filled symbols
869 correspond to the upward and downward moving target, respectively. To illustrate the influence
870 of target speed, the post-injection horizontal average position/time landing of saccades to the
871 10°/s and 40°/s targets is plotted as a function of the average values obtained with the 20°/s
872 target (panel C). Diagonal gray lines correspond to equality between abscissae and ordinate
873 values.

874

875 Fig. 5. Comparing the effects on horizontal and vertical saccades. The post-injection average
876 values of horizontal position/time landing of vertical saccades are plotted as a function of the
877 ipsilesional (panel A) and contralesional (panel B) position/time landing of horizontal saccades
878 (previously described in Burrelly et al. 2018a) for each experiment and each monkey (square
879 symbols: monkey A; circle symbols: monkey Bi). The panel C shows the horizontal
880 position/time landing of vertical saccades after muscimol injection as a function of the net
881 bilateral effect on horizontal saccades (difference of ipsilesional and contralesional horizontal
882 position/ time landing ratios). The light gray, dark gray and black symbols correspond to the
883 10, 20 and 40°/s target speeds, respectively. Open and filled symbols correspond to the upward
884 and downward moving target, respectively.

885

886 Fig. 6. Landing position and time of saccades toward a target moving with a non-constant speed
887 along the vertical meridian. The horizontal landing positions are plotted as a function of the
888 landing times for saccades made toward an accelerating (A, B and C) or decelerating (D, E and
889 F) target, before (open symbols) and after (filled symbols) muscimol injection. Black and gray
890 symbols correspond to the upward and downward moving target, respectively. The dashed lines
891 show the horizontal target position.

892

893 Fig. 7. Position/time landing of saccades toward a target moving along the vertical meridian
894 with a non-constant speed. The average values of the vertical (panel A) and horizontal (panel
895 B) component were calculated for the pre- and post-injection sessions of each experiment and
896 plotted for each monkey (square symbols: monkey A; circle symbols: monkey Bi). The gray
897 and black symbols correspond to the accelerating and decelerating target, respectively. Open
898 and filled symbols correspond to the upward and downward moving target, respectively. To

899 illustrate the effect of target speed, the post-injection horizontal average position/time landing
900 of saccades to the accelerating and decelerating targets is plotted as a function of the values
901 obtained with the 20°/s target (constant speed) (panel C). Diagonal gray lines correspond to
902 unity lines.

903

904 Fig. 8. Horizontal landing position of saccades toward a target moving along the vertical
905 meridian. The horizontal landing positions are plotted as a function of the vertical amplitude
906 after muscimol injection in the left cFN in monkey A (A and B: experiments A2 and A3) and
907 monkey Bi (C and D: experiments Bi7 and Bi8). The light gray, dark gray and black symbols
908 correspond to the 10, 20 and 40°/s target speed, respectively. Open and filled symbols
909 correspond to the upward and downward moving target, respectively. The relation obtained
910 with saccades toward a target moving with changing speeds are shown in the insets (gray
911 symbols: constant speeds, black symbols: changing speeds).

912 Fig. 9. Pathophysiology of the ipsipulsion of vertical saccades after muscimol injection in the
913 right caudal fastigial nucleus. The arrows correspond to excitatory connections whereas the
914 connecting lines ended by a circle depict inhibitory connections. The gray stain illustrates the
915 muscimol spread. MR: medial rectus; LR: lateral rectus; MNs: motoneurons; INs: internuclear
916 neurons; EBNs and IBNs: excitatory and inhibitory burst neurons; SFNs: saccade-related
917 fastigial neurons. See text for detailed explanation.

918

919 **Legends of tables**

920 Table 1. Relation between horizontal landing position and both vertical saccade duration and
921 amplitude after cFN inactivation (target moving at constant speed). Values are the slope, y
922 intercepts and coefficient of determination of the regression lines that fit the relationship
923 between the horizontal landing position and the vertical amplitude or duration of saccades
924 toward a target moving at constant speed (upward and downward movement pooled together).
925 Injections are labeled as defined in the text. The side and volume of injection are also indicated.
926 Bold numerical values correspond to statistically significant correlations ($P < 0.05$).

927

928 Table 2. Relation between horizontal landing position and both vertical saccade duration and
929 amplitude after cFN inactivation (accelerating and decelerating target). Values are the slope, y
930 intercepts, and coefficient of determination of the regression lines that fit the relationships
931 between horizontal landing position and the vertical amplitude and duration of saccades toward
932 a target moving with an increasing speed (from 0 to 40°/s, accelerating target) or decreasing
933 speed (from 40 to 0°/s, decelerating target). Upward and downward movement are pooled
934 together. Injections are labeled as defined in the text. The side and volume of injection are also
935 indicated. Bold numerical values correspond to statistically significant correlations ($P < 0.05$).

936

937

938 **Acknowledgements:**

939 Supported by the Centre National de la Recherche Scientifique, this work received funding
940 from the European Research Council under the European Union's Seventh Framework
941 Programme (FP7/2007-2013/ERC grant agreement no. AG324070 with Patrick Cavanagh) and
942 from the Agence Nationale de la Recherche (Grant VISAFIX). This work was also made
943 possible thanks to a support from the Fondation pour la Recherche Médicale
944 (FDT20160435585) to CB, and from the Fondation de France (Berthe Fouassier 0039352) to
945 JQ. The authors thank Dr Paul May for his corrections and suggestions for clarification, Marc
946 Martin, Luc Renaud for outstanding zootechnical and surgical assistance, Xavier Degiovanni
947 and Joël Baurberg for technical assistance, Ivan Balansard for veterinarian surveillance, and Dr
948 Ivo Vanzetta for kindly lending us one monkey (Bi).

Fig. 1

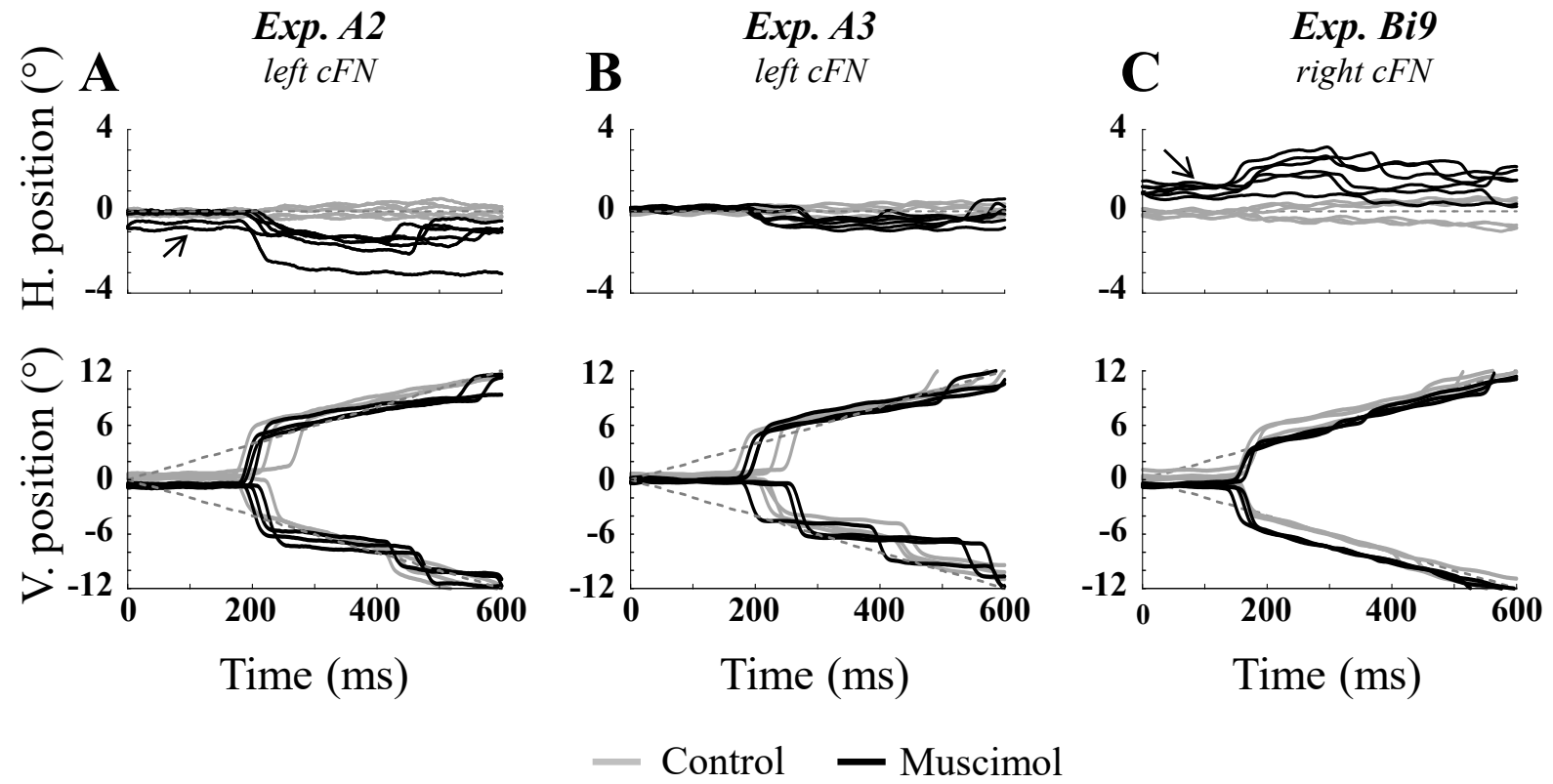


Fig. 2

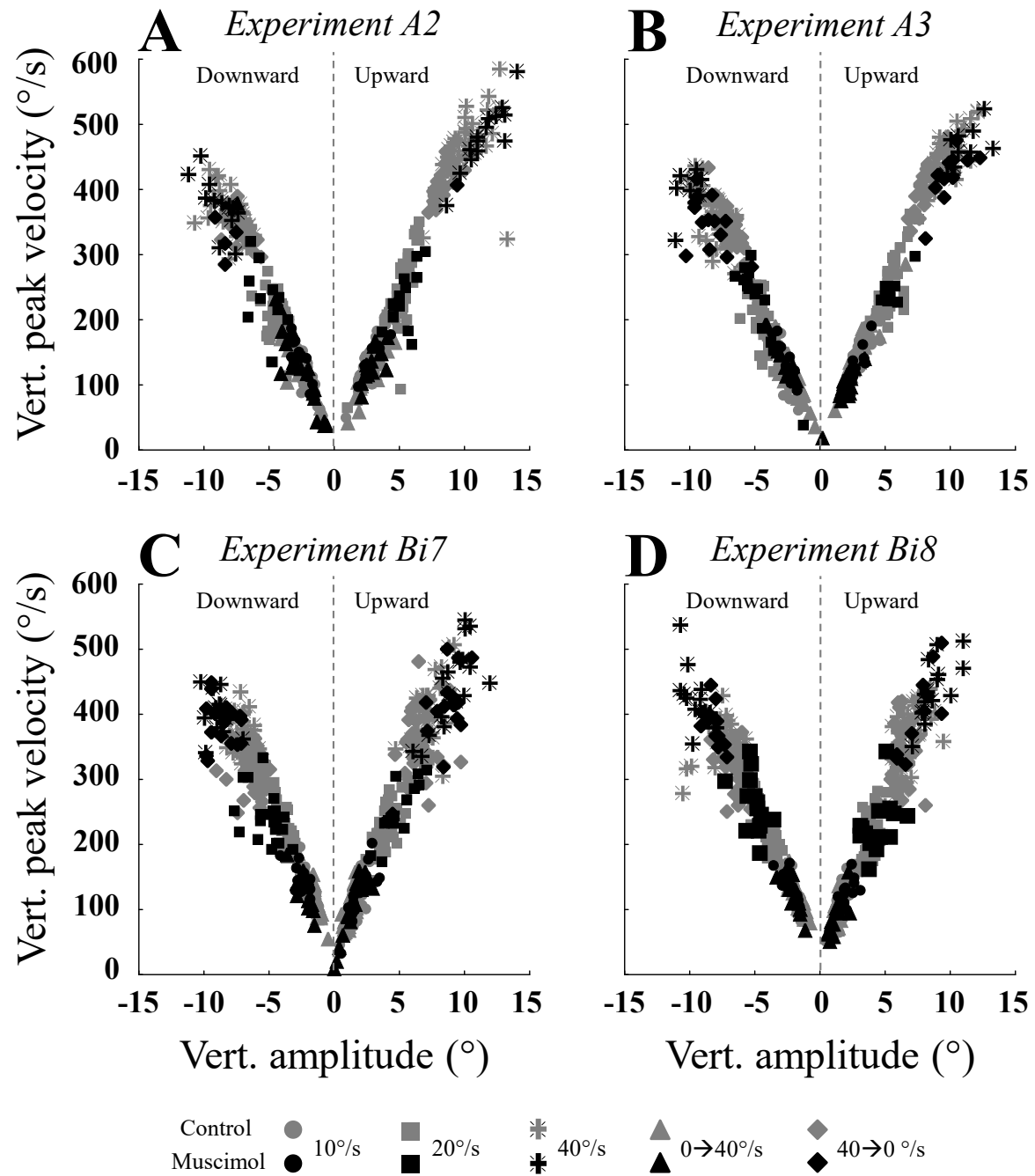


Fig. 3

Constant target speed

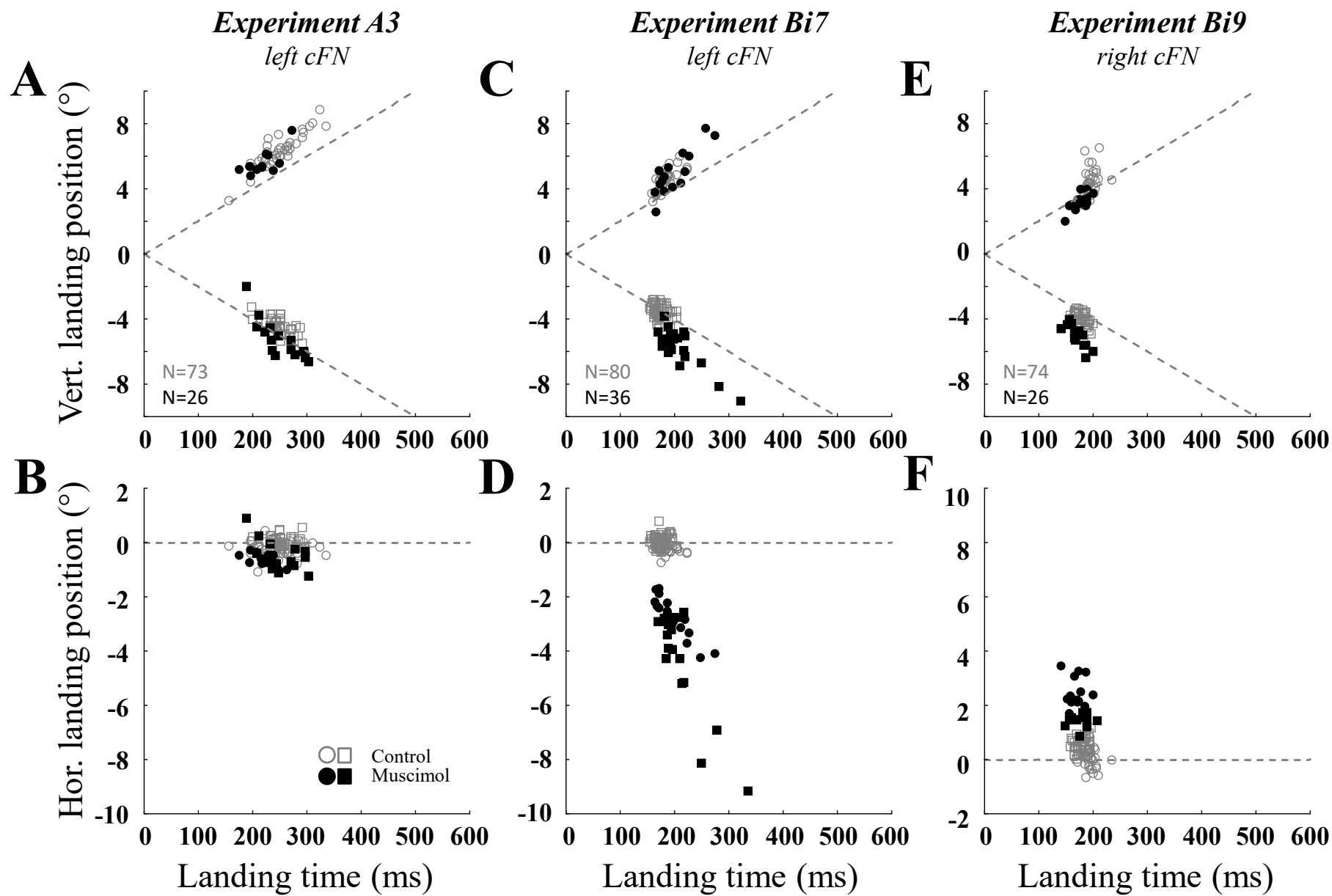


Fig. 4

Constant target speed

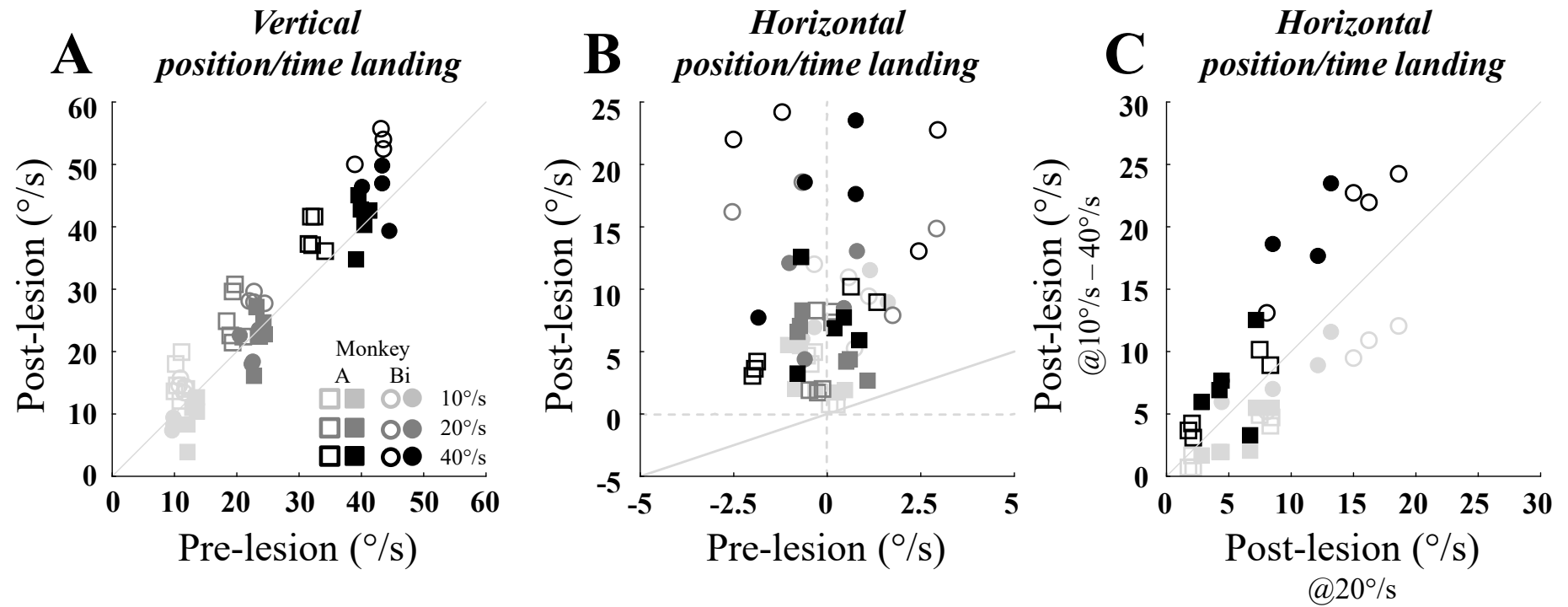


Fig. 5

Constant target speed

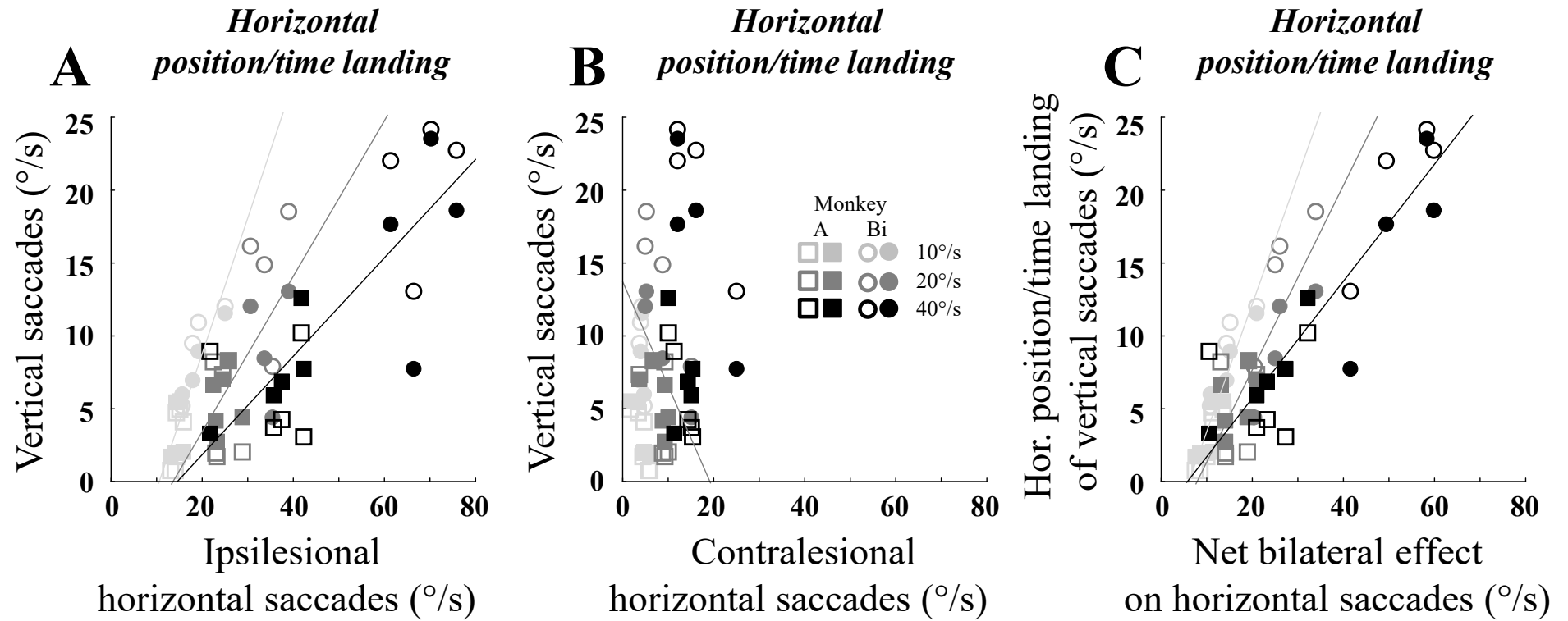


Fig. 6

Changing target speed

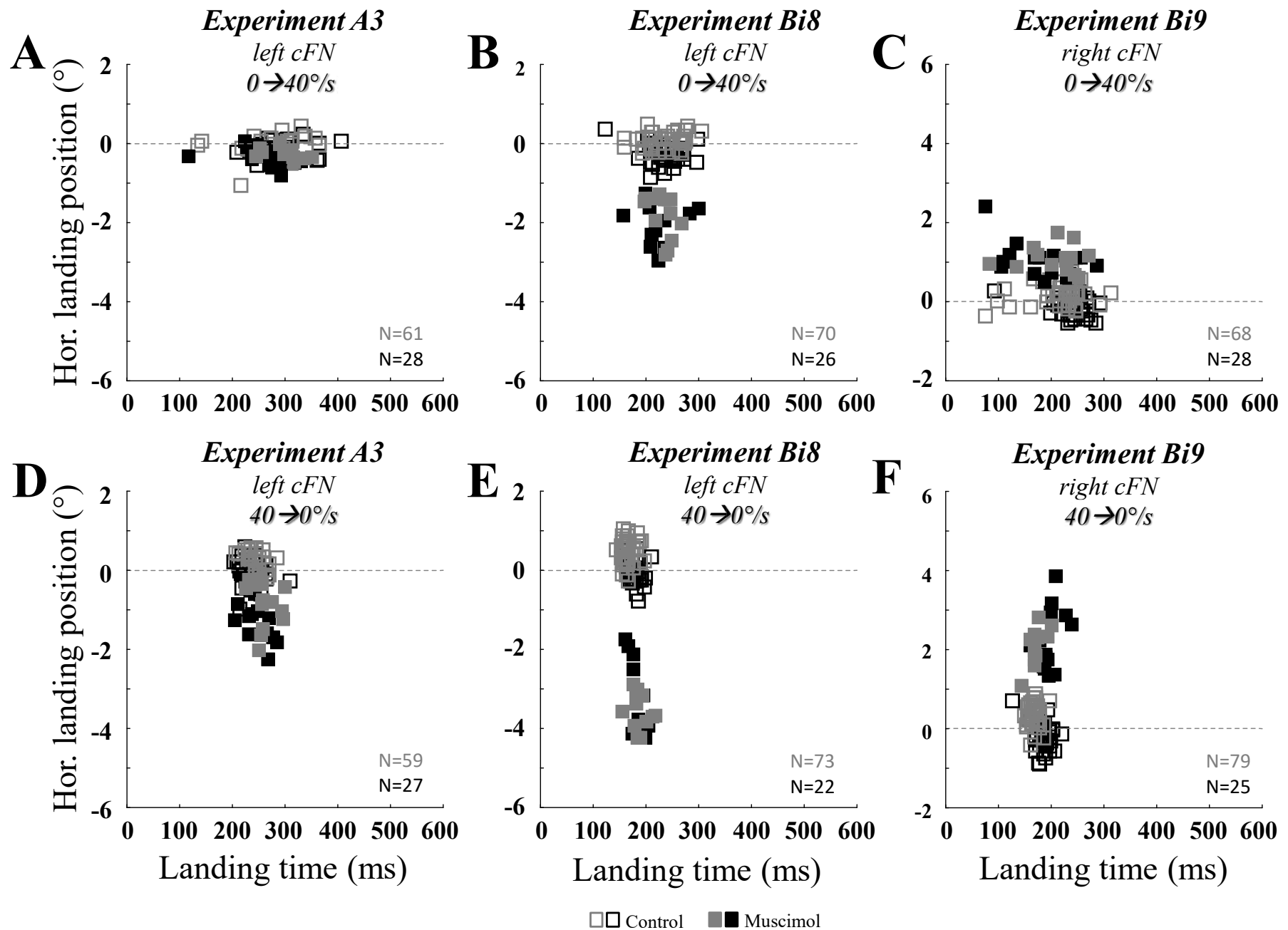


Fig. 7

Changing target speed

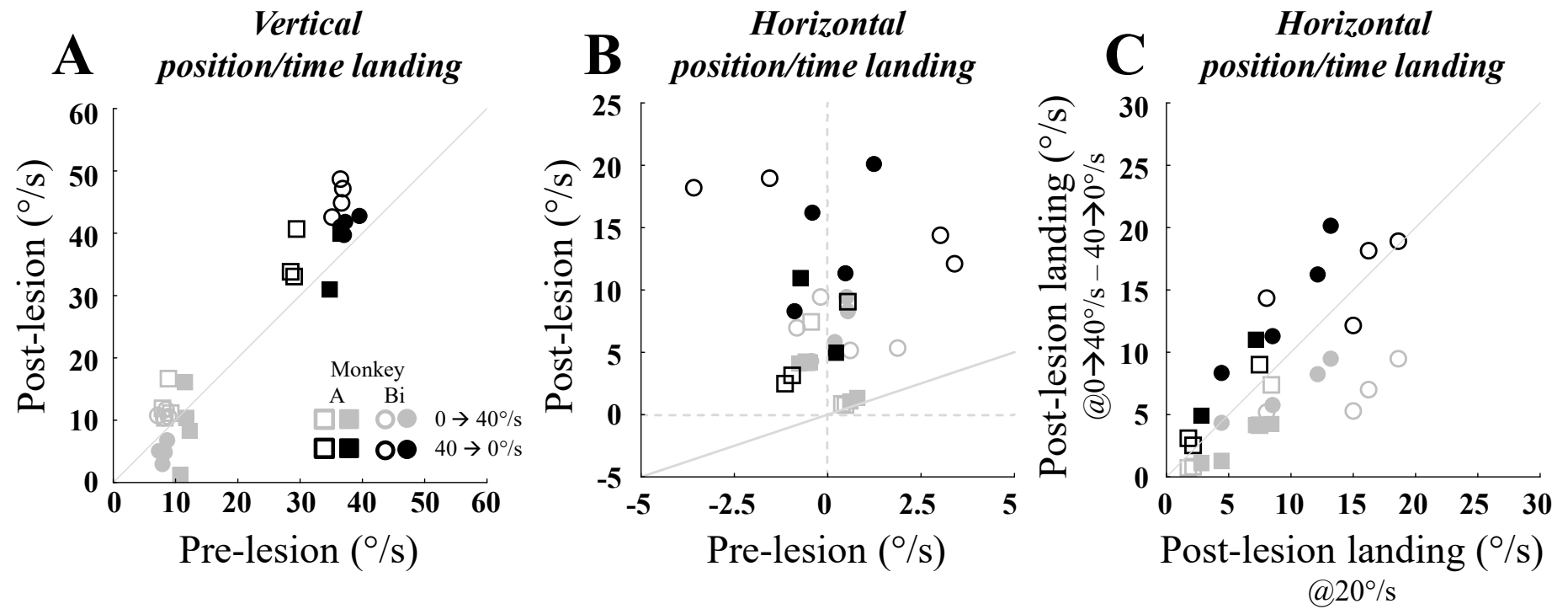


Fig. 8

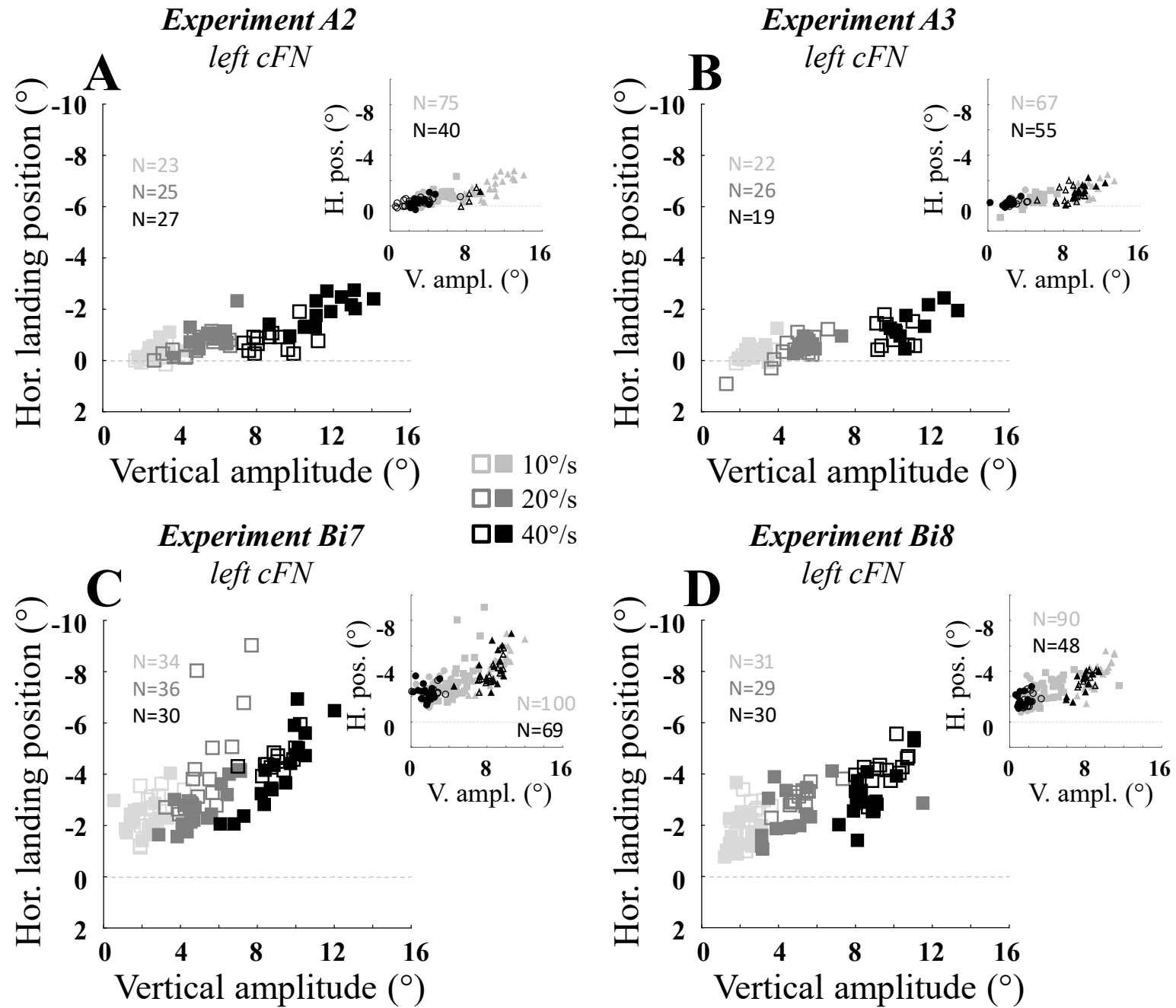


Figure 9

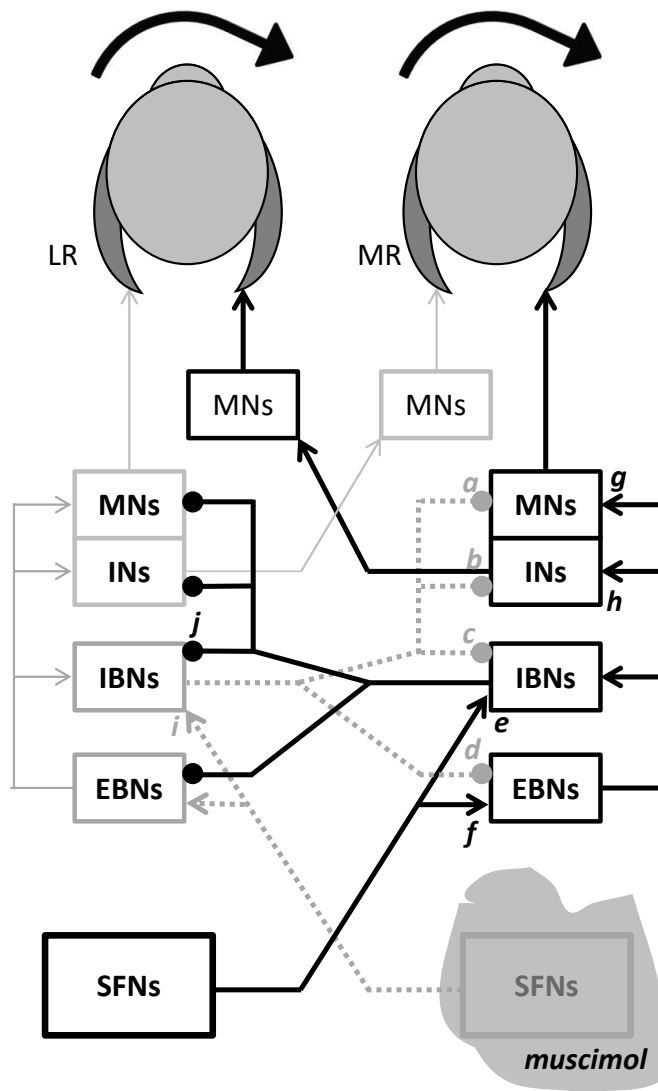


Table 1

| Exp | injection | | 10°/s | | | | 20°/s | | | | 40°/s | | | |
|------|---------------------|-----------|-----------|-------------|---------------|----------------|-----------|-------------|---------------|----------------|-----------|-------------|---------------|----------------|
| | | | N | Y-int | slope | R ² | N | Y-int | slope | R ² | N | Y-int | slope | R ² |
| A1 | Left cFN 1.0 µl | Amplitude | 18 | -0.2 | -0.108 | 0.09 NS | 38 | -0.0 | -0.132 | 0.26* | 20 | 1.1 | -0.239 | 0.48* |
| | | Duration | 18 | -0.5 | -0.001 | 0.001 NS | 38 | 0.3 | -0.028 | 0.14* | 20 | 1.6 | -0.067 | 0.52* |
| A2 | Left cFN 0.5 µl | Amplitude | 23 | 0.2 | -0.185 | 0.15 NS | 25 | 0.7 | -0.281 | 0.42* | 27 | 1.9 | -0.327 | 0.65* |
| | | Duration | 23 | -0.1 | -0.009 | 0.01 NS | 25 | -0.2 | -0.014 | 0.07 NS | 27 | 1.5 | -0.065 | 0.17* |
| A3 | Left cFN 0.3 µl | Amplitude | 22 | 0.4 | -0.278 | 0.33* | 26 | 1.1 | -0.328 | 0.66* | 19 | 1.7 | -0.284 | 0.29* |
| | | Duration | 22 | 0.4 | -0.024 | 0.10 NS | 26 | 0.6 | -0.031 | 0.06 NS | 19 | -1.0 | -0.005 | 0.003 NS |
| A4 | Right cFN 1.1 µl | Amplitude | 30 | 1.3 | 0.055 | 0.001 NS | 26 | 2.4 | -0.062 | 0.003 NS | - | - | - | - |
| | | Duration | 30 | -0.9 | 0.070 | 0.08 NS | 26 | 0.7 | 0.034 | 0.03 NS | - | - | - | - |
| A5 | Right cFN 1.0 µl | Amplitude | 15 | 2.5 | -0.411 | 0.29* | 28 | 1.5 | 0.044 | 0.00 NS | 18 | 5.7 | -0.413 | 0.31* |
| | | Duration | 15 | 3.1 | -0.069 | 0.10 NS | 28 | 1.5 | 0.005 | 0.00 NS | 18 | 1.9 | -0.007 | 0.002 NS |
| A6 | Right cFN 0.5 µl | Amplitude | 26 | 0.6 | 0.252 | 0.18* | 24 | 0.5 | 0.207 | 0.26* | 26 | -0.1 | 0.312 | 0.53* |
| | | Duration | 26 | 0.5 | 0.026 | 0.13 NS | 24 | 0.8 | 0.019 | 0.11 NS | 26 | -0.1 | 0.066 | 0.36* |
| Bi7 | Left cFN 0.2 µl | Amplitude | 34 | -1.6 | -0.355 | 0.15* | 36 | 1.0 | -0.889 | 0.41* | 30 | 2.6 | -0.772 | 0.67* |
| | | Duration | 34 | -0.5 | -0.078 | 0.28* | 36 | 3.2 | -0.198 | 0.37* | 30 | -1.8 | -0.066 | 0.09 NS |
| Bi8 | Left cFN 0.2 µl | Amplitude | 31 | -0.9 | -0.522 | 0.18* | 29 | -1.7 | -0.209 | 0.18* | 30 | 2.7 | -0.701 | 0.56* |
| | | Duration | 31 | 0.1 | -0.088 | 0.30* | 29 | -0.5 | -0.073 | 0.28* | 30 | -0.6 | -0.078 | 0.14* |
| Bi9 | Right cFN 0.5 µl | Amplitude | 24 | 0.8 | 0.338 | 0.22* | 26 | -0.2 | 0.576 | 0.34* | 24 | 3.1 | 0.061 | 0.00 NS |
| | | Duration | 24 | 1.0 | 0.021 | 0.07 NS | 26 | -0.3 | 0.081 | 0.11 NS | 24 | 3.4 | 0.006 | 0.00 NS |
| Bi10 | Right cFN 0.2 µl | Amplitude | 28 | 1.3 | -0.130 | 0.02 NS | 28 | -0.3 | 0.351 | 0.23* | 26 | 0.8 | 0.120 | 0.02 NS |
| | | Duration | 28 | 0.5 | 0.023 | 0.06 NS | 28 | 0.7 | 0.013 | 0.01 NS | 26 | 2.0 | -0.005 | 0.00 NS |

Table 2

| Exp | injection | | Accelerating target | | | | Decelerating target | | | |
|------|---------------------|-----------|---------------------|-------------|---------------|----------------|---------------------|-------------|---------------|----------------|
| | | | N | Y-int | slope | R ² | N | Y-int | slope | R ² |
| A2 | Left cFN 0.5 µl | Amplitude | 35 | 0.0 | -0.131 | 0.34* | 5 | 4.9 | -0.663 | 0.74 NS |
| | | Duration | 35 | 0.0 | -0.012 | 0.06 NS | 5 | -0.8 | 0.001 | 0.00 NS |
| A3 | Left cFN 0.3 µl | Amplitude | 28 | -0.0 | -0.104 | 0.18* | 27 | 1.1 | -0.233 | 0.31* |
| | | Duration | 28 | 0.2 | -0.016 | 0.15* | 27 | -0.5 | -0.012 | 0.04 NS |
| A4 | Right cFN 1.1 µl | Amplitude | 15 | 2.7 | -0.196 | 0.10 NS | - | - | - | - |
| | | Duration | 15 | 3.1 | -0.034 | 0.06 NS | - | - | - | - |
| A6 | Right cFN 0.5 µl | Amplitude | 24 | 0.7 | 0.215 | 0.29* | 27 | 0.4 | 0.231 | 0.39* |
| | | Duration | 24 | 0.4 | 0.026 | 0.14 NS | 27 | 1.1 | 0.027 | 0.14 NS |
| Bi7 | Left cFN 0.2 µl | Amplitude | 35 | -2.3 | 0.016 | 0.00 NS | 34 | 0.9 | -0.581 | 0.34* |
| | | Duration | 35 | -1.8 | -0.019 | 0.04 NS | 34 | -0.7 | -0.088 | 0.25* |
| Bi8 | Left cFN 0.2 µl | Amplitude | 26 | -1.4 | -0.205 | 0.06 NS | 22 | 1.5 | -0.594 | 0.55* |
| | | Duration | 26 | -0.4 | -0.063 | 0.32* | 22 | -1.3 | -0.052 | 0.10 NS |
| Bi9 | Right cFN 0.5 µl | Amplitude | 28 | 1.0 | 0.013 | 0.00 NS | 25 | -0.3 | 0.310 | 0.33* |
| | | Duration | 28 | 1.0 | 0.002 | 0.00 NS | 25 | 0.7 | 0.039 | 0.17* |
| Bi10 | Right cFN 0.2 µl | Amplitude | 29 | 0.9 | 0.115 | 0.04 NS | 22 | -2.2 | 0.537 | 0.12* |
| | | Duration | 29 | 0.7 | 0.016 | 0.04 NS | 22 | 3.7 | -0.04 | 0.05 NS |